

Numerical solution of parametrized Navier-Stokes equations by reduced basis methods

Alfio Quarteroni ^{‡,§}, Gianluigi Rozza ^{§*}

September 24, 2006

[‡]Modellistica e Calcolo Scientifico (MOX),
Dipartimento di Matematica “F.Brioschi”,
Politecnico di Milano,
20133 Milano, Italy.

[§]Modelling and Scientific Computing (CMCS),
Institute of Analysis and Scientific Computing (IACS),
EPFL, École Polytechnique Fédérale de Lausanne,
Station 8, CH-1015, Lausanne, Switzerland.
alfio.quarteroni@epfl.ch, gianluigi.rozza@epfl.ch

Key words: *Navier-Stokes parametrized equations; reduced-basis methods; Galerkin approximation; numerical stability; inf-sup condition; supremizer; empirical interpolation.*

Abstract

We apply the reduced basis method to solve Navier-Stokes equations in parametrized domains. Special attention is devoted to the treatment of the parametrized non-linear transport term in the reduced basis framework, including the case of non-affine parametric dependence that is treated by an empirical interpolation method. This method features *(i)* a rapid global convergence owing to the property of the Galerkin projection onto a space W_N spanned by solutions of the governing partial differential equation at N (optimally) selected points in the parameter space, and *(ii)* the off-line/on-line computational procedures which decouple the generation and projection stages of the approximation process.

This method is well suited for the repeated and rapid evaluations required

*currently at MIT, Mech.Eng.Dpt., room 3-264, 77 Mass Avenue, 02142 Cambridge MA (USA), rozza@mit.edu.

in the context of parameter estimation, design, optimization, and real-time control. Our analysis focuses on: (i) the pressure treatment of incompressible Navier-Stokes problem; (ii) the fulfillment of an equivalent *inf-sup* condition to guarantee the stability of the reduced basis solutions. The applications that we consider involve parametrized geometries, like e.g. a channel with curved upper wall or an arterial bypass configuration.

1 Introduction

The use of reduced basis methods in numerical fluid dynamics is aimed at providing real-time solutions and information on fluid mechanics outputs. Their extension to the non-linear steady Navier-Stokes equations which requires treatment of non-linearities and non-affine parametric dependence, provides an efficient optimization toolbox in design problems with a certain degree of complexity.

Previous works on reduced basis methods for non-linear problems in fluid mechanics were carried out in the 1990s by Peterson [17] and by Ito and Ravindran [12]. The former work was focused on stream-function and vorticity formulation for various Reynolds numbers; either Taylor and Lagrangian basis functions were used to build the approximation space. In the latter the authors built a reduced basis approximation for a Navier-Stokes problem (either steady or unsteady) in a cavity using different techniques to build reduced basis approximation spaces (Hermite and/or Taylor spaces, incorporating the derivatives of velocity with respect to the considered parameter, the Reynolds number). In this case the reduced basis formulation does not include the pressure in the reduced-order model. More recently Patera and Veroy, have developed the reduced basis in non-linear fluid mechanics using Lagrangian basis (i.e. global approximation functions) to study natural convection problem, parametrized by physical quantities (such as the Grashof number [15] or the viscosity [35]) in divergence-free spaces. In [34] they developed rigorous a posteriori error estimation and bounds for real time computation based on the *Brezzi-Rappaz-Raviart* theory. A review is provided also in [8]. In our work we follow this line and focus our attention on the following aspects: i) the efficient treatment of the non-linear term; ii) the domain parametrization; iii) the incorporation of a stable approximation for pressure (useful for example in haemodynamic applications, see [28]); iv) the use of non-affine transformation terms by an empirical interpolation method to allow for more complex geometries, such as curved walls. Related aspects deal with the use of different options to build the reduced basis velocity spaces and the efficient off-line selection of the basis functions.

Recent results address flow optimization using sensitivity analysis and the reduced basis method, see for example Burkardt [3] and Gunzburger [11]. A reduced basis element method has been proposed by Løvgrén *et al.* to solve steady Navier-Stokes problems with geometrical parameters [14].

The present work is organized as follows: after this introduction, we have made a short review on the use of reduced basis for Navier-Stokes, then in Section 2

the formulation of the steady Navier-Stokes problem is presented. From Section 3 to Section 5 we build the reduced basis formulation for Navier-Stokes equations in parametrized domains with (i) affine, (ii) non-affine and (iii) combined affine/non-affine parametric dependence. Several aspects relevant to algebraic and approximation stability are analyzed. In particular, we consider the problem of ill-conditioning and the choice of the basis, by exploring algorithms to optimize the selection of basis functions for chosen values of parameters and, possibly, orthonormalization procedures for the basis functions. Moreover, we focus on the problem of fulfilling an equivalent inf-sup condition to guarantee the stability of the pressure solution. In Sections 6, 7 and 8 numerical results and computational costs and savings are reported. Some conclusions follow.

2 Steady Navier-Stokes equations

The steady Navier-Stokes equations in a domain $\Omega \subset \mathbb{R}^d (d = 1, 2, 3)$ with mixed boundary conditions on $\Gamma = \Gamma_{in} \cup \Gamma_{out} \cup \Gamma_w$ read:

$$\begin{cases} -\nu \Delta \mathbf{u} + (\mathbf{u} \cdot \nabla) \mathbf{u} + \nabla p = \mathbf{f} \text{ in } \Omega, \\ \nabla \cdot \mathbf{u} = 0 \text{ in } \Omega, \\ \mathbf{u} = \mathbf{0} \text{ on } \Gamma_w, \mathbf{u} = \mathbf{g}_{in} \text{ on } \Gamma_{in}, \left(\nu \frac{\partial \mathbf{u}}{\partial \mathbf{n}} - p \hat{\mathbf{n}} \right) = \mathbf{0} \text{ on } \Gamma_{out}, \end{cases} \quad (2.1)$$

where Ω is a domain occupied by fluid of constant density, \mathbf{u} is the fluid velocity, p the pressure, \mathbf{f} a force field, ν a kinematic viscosity and \mathbf{n} the normal unit vector to the domain boundary. For the mathematical theory of the Navier-Stokes equations see e.g. Galdi [6] and for their numerical solution see Temam [33], Girault and Raviart [7], Brezzi and Fortin [2], Canuto *et al.* [5].

The weak formulation of problem (2.1) reads: find $\mathbf{u} \in Y = (H_{\Gamma_D}^1(\Omega))^d$, $p \in Q = L^2(\Omega)$:

$$\begin{cases} \nu \int_{\Omega} \nabla \mathbf{u} \cdot \nabla \mathbf{w} d\Omega - \int_{\Omega} p \nabla \cdot \mathbf{w} d\Omega + \int_{\Omega} (\mathbf{u} \cdot \nabla) \mathbf{u} \cdot \mathbf{w} d\Omega = \int_{\Omega} \mathbf{f} \cdot \mathbf{w} d\Omega + \langle F^0, \mathbf{w} \rangle \quad \forall \mathbf{w} \in Y, \\ \int_{\Omega} q \nabla \cdot \mathbf{u} d\Omega = \langle G^0, q \rangle \quad \forall q \in Q, \end{cases} \quad (2.2)$$

F^0, G^0 are terms due to non-homogeneous Dirichlet boundary condition on Γ_{in} , $\Gamma_D = \Gamma_{in} \cup \Gamma_w$ and $H_{\Gamma_D}^1(\Omega) = \{v \in H^1(\Omega) : v = 0 \text{ on } \Gamma_D\}$. If Γ_{out} is empty, then Q must be taken as $L_0^2(\Omega) = \{q \in L^2(\Omega) : \int_{\Omega} q = 0\}$. We discretize problem (2.2) by a stable finite element approximation (e.g. the Taylor-Hood $\mathbb{P}^2 - \mathbb{P}^1$ elements for velocity and pressure, respectively) on a fine mesh triangulation; see, for example, Quarteroni and Valli [21] and Gresho and Sani [9]. To solve the system of non-linear equations arising from the space discretization of (2.2) we use the iterative (quadratically convergent) Newton method [22] which involves the Frechet linearization of the advection term $(\mathbf{u}_h \cdot \nabla) \mathbf{u}_h$. The linearized version

of the discretized problem (2.2) at each iteration reads: for $k \geq 0$, given $\mathbf{u}_h^{(k)}$, find $\mathbf{u}_h^{(k+1)} \in Y_h$, $p_h^{(k+1)} \in Q_h$, such that

$$\left\{ \begin{array}{l} \nu \int_{\Omega} \nabla \mathbf{u}_h^{(k+1)} \cdot \nabla \mathbf{w}_h d\Omega - \int_{\Omega} p_h^{(k+1)} \nabla \cdot \mathbf{w}_h d\Omega + \int_{\Omega} [(\mathbf{u}_h^{(k)} \cdot \nabla) \mathbf{u}_h^{(k+1)} + \\ + (\mathbf{u}_h^{(k+1)} \cdot \nabla) \mathbf{u}_h^{(k)}] \cdot \mathbf{w}_h d\Omega - \int_{\Omega} (\mathbf{u}_h^{(k)} \cdot \nabla) \mathbf{u}_h^{(k)} \cdot \mathbf{w}_h d\Omega = \\ = \int_{\Omega} \mathbf{f} \cdot \mathbf{w}_h d\Omega + \langle F^0, \mathbf{w}_h \rangle \quad \forall \mathbf{w}_h \in Y_h, \\ \int_{\Omega} q_h \nabla \cdot \mathbf{u}_h^{(k+1)} d\Omega = \langle G^0, q_h \rangle \quad \forall q_h \in Q_h, \end{array} \right. \quad (2.3)$$

where Y_h and Q_h are stable finite element subspaces of Y and Q respectively. As stopping criterium we can adopt a condition based on the difference between two steps

$$\|\mathbf{u}_h^{(k+1)} - \mathbf{u}_h^{(k)}\| \leq \epsilon$$

where ϵ is a given (small) tolerance. To solve the linearized Navier-Stokes system (2.3) at each Newton step we can use the *Pressure Matrix Method* to decouple the calculation of pressure from the velocity field. The problem is solved in three steps: we first compute an auxiliary velocity $\tilde{\mathbf{u}}_h$, which is not divergence-free, then we can calculate the pressure p_h and then in the third step the corrected velocity \mathbf{u}_h^{k+1} is recovered. See for example Quarteroni and Valli [21].

3 Parametrized formulation: affine parametric dependence

We suppose that the domain we are considering is made of R parametrized components: $\hat{\Omega} = (\bigcup_{r=1}^R \hat{\Omega}^r)$, so that we rewrite (2.3) as follows, introducing the “hat” to indicate equations in parametrized domains and dropping the subscript h on the unknowns and test functions for simplicity of notation:

$$\left\{ \begin{array}{l} \hat{\mathcal{A}}(\hat{\mathbf{u}}^{(k+1)}, \hat{\mathbf{w}}) + \hat{\mathcal{B}}(\hat{p}^{(k+1)}, \hat{\mathbf{w}}) + \hat{\mathcal{C}}(\hat{\mathbf{u}}^{(k+1)}, \hat{\mathbf{u}}^{(k)}, \hat{\mathbf{w}}) + \hat{\mathcal{C}}(\hat{\mathbf{u}}^{(k)}, \hat{\mathbf{u}}^{(k+1)}, \hat{\mathbf{w}}) = \\ = \langle \hat{F}, \hat{\mathbf{w}} \rangle + \hat{\mathcal{C}}(\hat{\mathbf{u}}^{(k)}, \hat{\mathbf{u}}^{(k)}, \hat{\mathbf{w}}) \quad \forall \hat{\mathbf{w}} \in \hat{Y}_h, \\ -\hat{\mathcal{B}}(\hat{q}, \hat{\mathbf{u}}^{(k+1)}) = \langle \hat{G}^0, \hat{q} \rangle \quad \forall \hat{q} \in \hat{Q}_h, \end{array} \right. \quad (3.4)$$

where for $1 \leq i, j \leq d$ and $\hat{\nu}_{i,j} = \nu \delta_{i,j}$ (summation convention is understood):

$$\hat{\mathcal{A}}(\hat{\mathbf{u}}, \hat{\mathbf{w}}) = \sum_{r=1}^R \int_{\hat{\Omega}^r} \frac{\partial \hat{\mathbf{u}}}{\partial \hat{x}_i} \hat{\nu}_{ij} \frac{\partial \hat{\mathbf{w}}}{\partial \hat{x}_j} d\hat{\Omega}, \quad (3.5)$$

$$\hat{\mathcal{B}}(\hat{p}, \hat{\mathbf{w}}) = - \sum_{r=1}^R \int_{\hat{\Omega}^r} \hat{p} \nabla \cdot \hat{\mathbf{w}} d\hat{\Omega}, \quad (3.6)$$

$$\hat{\mathcal{C}}(\hat{\mathbf{u}}, \hat{\mathbf{v}}, \hat{\mathbf{w}}) = \sum_{r=1}^R \int_{\hat{\Omega}^r} (\hat{\mathbf{u}} \cdot \nabla) \hat{\mathbf{v}} \cdot \hat{\mathbf{w}} d\hat{\Omega}, \quad (3.7)$$

$$\langle \hat{F}, \hat{\mathbf{w}} \rangle = \langle \hat{F}_s, \hat{\mathbf{w}} \rangle + \langle \hat{F}^0, \hat{\mathbf{w}} \rangle, \quad (3.8)$$

with

$$\langle \hat{F}_s, \hat{\mathbf{w}} \rangle = \sum_{r=1}^R \int_{\hat{\Omega}^r} \hat{\mathbf{f}} \hat{\mathbf{w}} d\hat{\Omega}, \langle \hat{F}^0, \hat{\mathbf{w}} \rangle = -\langle \hat{\mathcal{A}} \hat{\mathbf{g}}_{in}, \hat{\mathbf{w}} \rangle, \langle \hat{G}^0, \hat{q} \rangle = \langle \hat{\mathcal{B}} \hat{q}, \hat{\mathbf{g}}_{in} \rangle. \quad (3.9)$$

Now we want to build a system of P^2DEs (*Parametrized Partial Differential Equations*) affinely depending on a set of geometrical parameters (μ) , to be specified later. Problem (3.4) is traced back to a *reference domain* by an *affine mapping* on subdomains $\hat{\Omega}^r$ into Ω^r . For any $\hat{x} \in \hat{\Omega}^r$, $r = 1, \dots, R$, its image $x \in \Omega^r$ is given by

$$x = \mathcal{G}^r(\mu; \hat{x}) = G^r(\mu) \hat{x} + g^r, \quad 1 \leq r \leq R; \quad (3.10)$$

we thus write on Ω_r

$$\frac{\partial}{\partial \hat{x}_i} = \frac{\partial x_j}{\partial \hat{x}_i} \frac{\partial}{\partial x_j} = G_{ji}^r(\mu) \frac{\partial}{\partial x_j}. \quad (3.11)$$

The discretized P^2DEs system depending on μ on the reference domain Ω reads: for $k \geq 0$, given $\mathbf{u}^{(k)}$, find $\mathbf{u}^{(k+1)} \in Y = (H_{\Gamma_D}^1(\Omega))^d$, $p^{(k+1)} \in Q = L^2(\Omega)$:

$$\begin{cases} \mathcal{A}(\mu; \mathbf{u}^{(k+1)}, \mathbf{w}) + \mathcal{B}(\mu; p^{(k+1)}, \mathbf{w}) + \mathcal{C}(\mu; \mathbf{u}^{(k+1)}, \mathbf{u}^{(k)}, \mathbf{w}) + \mathcal{C}(\mu; \mathbf{u}^{(k)}, \mathbf{u}^{(k+1)}, \mathbf{w}) = \\ \langle F_s + F^0, \mathbf{w} \rangle + \mathcal{C}(\mu; \mathbf{u}^{(k)}, \mathbf{u}^{(k)}, \mathbf{w}) \quad \forall \mathbf{w} \in Y_h, \\ \mathcal{B}(\mu; q, \mathbf{u}^{(k+1)}) = \langle G^0, q \rangle \quad \forall q \in Q_h, \end{cases} \quad (3.12)$$

where:

$$\begin{aligned} \mathcal{A}(\mu, \mathbf{u}, \mathbf{w}) &= \sum_{r=1}^R \int_{\Omega^r} \frac{\partial \mathbf{u}}{\partial x_i} \nu_{ij}^r(\mu) \frac{\partial \mathbf{w}}{\partial x_j} d\Omega, \\ \mathcal{B}(\mu, p, \mathbf{w}) &= - \sum_{r=1}^R \int_{\Omega^r} p \chi_{ij}^r(\mu) \frac{\partial w_j}{\partial x_i} d\Omega, \\ \mathcal{C}(\mu, \mathbf{u}, \mathbf{v}, \mathbf{w}) &= - \sum_{r=1}^R \int_{\Omega^r} u_i \pi_{ij}^r(\mu) \frac{\partial v_j}{\partial x_i} \mathbf{w} d\Omega, \\ \langle F_s, \mathbf{w} \rangle &= \sum_{r=1}^R \int_{\Omega^r} \left(\hat{f}^r |(G^r(\mu))^{-1}| \right) \mathbf{w} d\Omega; \quad \langle F^0, \mathbf{w} \rangle = -\langle \mathcal{A} \mathbf{g}_{in}, \mathbf{w} \rangle; \\ \langle G^0, q \rangle &= \langle \mathcal{B} q, \mathbf{g}_{in} \rangle; \end{aligned}$$

the general formulation of the tensors for *viscous terms* is

$$\nu_{ij}^r(\mu) = G_{ii'}^r(\mu) \hat{\nu}_{i'j'} G_{jj'}^r(\mu) |(G^r(\mu))^{-1}|, \quad 1 \leq i, j \leq d, r = 1, \dots, R, \quad (3.13)$$

the one of the tensors for *pressure, divergence and convective terms* is:

$$\chi_{ij}^r(\mu) = \pi_{ij}^r(\mu) = G_{ij}^r |(G^r(\mu))^{-1}|, 1 \leq i, j \leq d, r = 1, \dots, R. \quad (3.14)$$

Using the affine decomposition property to exploit and decouple the on-line computational stage (many queries for different values of parameters) and the off-line one (computed once in the reference domain and then stored) we introduce the following elements:

$$\Theta^{q(i,j,r)}(\mu) = \nu_{ij}^r(\mu), \mathcal{A}^{q(i,j,r)}(\mathbf{u}, \mathbf{w}) = \int_{\Omega^r} \frac{\partial \mathbf{u}}{\partial x_i} \frac{\partial \mathbf{w}}{\partial x_j} d\Omega,$$

$$\Phi^{s(i,j,r)}(\mu) = \chi_{ij}^r(\mu), \mathcal{B}^{s(i,j,r)}(p, \mathbf{w}) = - \int_{\Omega^r} p \frac{\partial w_i}{\partial x_j} d\Omega,$$

$$\Upsilon^{s(i,j,r)}(\mu) = \pi_{ij}^r(\mu), \mathcal{C}^{s(i,j,r)}(\mathbf{u}, \mathbf{u}, \mathbf{w}) = \int_{\Omega^r} u_j \frac{\partial u_i}{\partial x_j} \mathbf{w} d\Omega,$$

$$\mathcal{A}(\Theta(\mu), \mathbf{u}, \mathbf{w}) = \sum_{q=1}^{Q^a} \Theta^q(\mu) \mathcal{A}(\mathbf{u}, \mathbf{w})^q;$$

$$\mathcal{B}(\Phi(\mu), p, \mathbf{w}) = \sum_{s=1}^{Q^b} \Phi^s(\mu) \mathcal{B}(p, \mathbf{w})^s;$$

$$\mathcal{C}(\Upsilon(\mu), \mathbf{u}, \mathbf{u}, \mathbf{w}) = \sum_{s=1}^{Q^c} \Upsilon^s(\mu) \mathcal{C}(\mathbf{u}, \mathbf{u}, \mathbf{w})^s;$$

where s and q are condensed indexes for i, j, r . If $\Omega \subset \mathbb{R}^d$, then $(Q^a) = d \times d \times d \times R$, $(Q^b) = d \times d \times R$ and $(Q^c) = d \times d \times d \times R$.

The reduced basis approximation for the Navier-Stokes system (3.12) reads: for $k \geq 0$, for a given $\mathbf{u}_N^{(k)}$ find $(\mathbf{u}_N^{(k+1)}(\mu), p_N^{(k+1)}(\mu)) \in Y_N \times Q_N$, such that

$$\begin{cases} \mathcal{A}(\mu; \mathbf{u}_N^{(k+1)}(\mu), \mathbf{w}) + \mathcal{B}(\mu; p_N^{(k+1)}(\mu), \mathbf{w}) + \mathcal{C}(\mu; \mathbf{u}_N^{(k+1)}(\mu), \mathbf{u}_N^{(k)}(\mu), \mathbf{w}) + \\ \mathcal{C}(\mu; \mathbf{u}_N^{(k)}(\mu), \mathbf{u}_N^{(k+1)}(\mu), \mathbf{w}) = \langle F, \mathbf{w} \rangle + \mathcal{C}(\mu; \mathbf{u}_N^{(k)}(\mu), \mathbf{u}_N^{(k)}(\mu), \mathbf{w}) \quad \forall \mathbf{w} \in Y_N, \\ \mathcal{B}(\mu; q, \mathbf{u}_N^{(k+1)}(\mu)) = \langle G, q \rangle \quad \forall q \in Q_N. \end{cases} \quad (3.15)$$

To build the global approximation space we select suitable samples called snapshots $\mu \in S_N^\mu = \{\mu^1, \dots, \mu^N\}$, where $\mu^n \in \mathcal{D}^\mu$, $n = 1, \dots, N$ and we solve N times the Navier-Stokes problem (3.12) using the Galerkin finite element method to obtain N solutions $\mathbf{u}_h(\mu^i)$ and $p_h(\mu^i)$, $i = 1, \dots, N$.

The *reduced basis pressure space* is:

$$Q_N = \text{span} \{ \xi_n, n = 1, \dots, N \}, \quad (3.16)$$

where $\xi_n = p_h(\mu^n)$. We now use the so-called *supremizer* solutions to enrich Y_N (as done for example in Rovas [23] and Patera *et al.* [15]). More precisely, the

reduced basis velocity space is given by:

$$\begin{aligned} Y_N &= \text{span} \{ \sigma_n, n = 1, \dots, 2N \} = \\ &= \text{span} \{ \zeta_n, T^{\mu^n} \xi_n, n = 1, \dots, N \}, \end{aligned} \quad (3.17)$$

where $\zeta_n = \mathbf{u}_h(\mu^n)$ and $T^{\mu^n}: Q_h \rightarrow Y_h$ is the supremizer operator defined by

$$(T^\mu q, \mathbf{w})_Y = \mathcal{B}(\mu; q, \mathbf{w}), \quad \forall \mathbf{w} \in Y_h. \quad (3.18)$$

We recall that we can write $T^{\mu^n} \xi = \sum_{q=1}^{Q^b} \Phi^q(\mu^n) T^q \xi$ for any ξ and μ^n thanks to affine composition property and the linearity of the supremizer operator.

Remark 3.1 *Note that in this case the reduced basis velocity space is depending on every value μ^n of the parameter used to compute the solution $\xi_n = p_h(\mu^n)$, considered as basis function. This procedure allows us to simplify the basis construction and to reduce the complexity of the problem, even if stability in this case can be proved only computationally (heuristic approach). \square*

Other options, for which stability can be theoretically proven, are available (see for example [24]) to get a different space Y_N for the velocity. For example: i) a space which is μ -independent, using only $T^q \xi$ components to enrich velocity space. This option is useful if we want to apply an orthonormalization procedure to restore algebraic stability; or ii) a space μ -dependent, using the online value of the parameter in Φ^q . Let us define the two *inf-sup* constants:

$$\beta_N(\mu) = \inf_{q \in Q_N} \sup_{\mathbf{w} \in Y_N} \frac{\mathcal{B}(\mu, q, \mathbf{w})}{\|\mathbf{w}\|_Y \|q\|_Q}, \quad (3.19)$$

and

$$\beta_h(\mu) = \inf_{q \in Q_h} \sup_{\mathbf{w} \in Y_h} \frac{\mathcal{B}(\mu, q, \mathbf{w})}{\|\mathbf{w}\|_Y \|q\|_Q}. \quad (3.20)$$

The former relates the reduced basis subspaces, the latter to the standard finite element spaces. Then it has been proven in [24] that

$$\beta_N(\mu) \geq \beta_h(\mu) \geq \beta_0 > 0, \quad \forall \mu \in \mathcal{D}^\mu. \quad (3.21)$$

For a new sample μ the reduced basis solution is built as:

$$\mathbf{u}_N(\mu) = \sum_{j=1}^{2N} u_{Nj}(\mu) \boldsymbol{\sigma}_j, \quad p_N(\mu) = \sum_{l=1}^N p_{Nl}(\mu) \xi_l.$$

The corresponding non-linear system becomes: for $1 \leq i, j, h \leq 2N$, $1 \leq l \leq N$,

$$\left\{ \begin{array}{l} \sum_{j=1}^{2N} A_{ij}^\mu \mathbf{u}_{Nj}^{(k+1)}(\mu) + \sum_{l=1}^N B_{il}^\mu p_{Nl}^{(k+1)}(\mu) + \sum_{h=1}^{2N} \sum_{j=1}^{2N} \mathbf{u}_{Nh}^{(k)}(\mu) C_{ijh}^\mu \mathbf{u}_{Nj}^{(k+1)}(\mu) + \\ + \sum_{h=1}^{2N} \sum_{j=1}^{2N} \mathbf{u}_{Nh}^{(k+1)}(\mu) C_{ijh}^\mu \mathbf{u}_{Nj}^{(k)}(\mu) = F_i^\mu + \sum_{h=1}^{2N} \sum_{j=1}^{2N} \mathbf{u}_{Nj}^{(k)}(\mu) C_{ijh}^\mu \mathbf{u}_{Nh}^{(k)}(\mu) \\ \sum_{j=1}^{2N} B_{jl}^\mu \mathbf{u}_{Nj}^{(k+1)}(\mu) = G_l^\mu, \quad 1 \leq l \leq N, \end{array} \right. \quad (3.22)$$

with

$$A_{ij}^\mu = \sum_{m=1}^{Q^a} \Theta^m(\mu) \mathcal{A}(\sigma_i, \sigma_j)^m, \quad B_{il}^\mu = \sum_{m=1}^{Q^b} \Phi^m(\mu) \mathcal{B}(\sigma_i, \xi_l)^m;$$

$$C_{ijh}^\mu = \sum_{m=1}^{Q^c} \Upsilon^m(\mu) \mathcal{C}(\sigma_h, \sigma_j, \sigma_i)^m;$$

$$F_i^\mu = \langle F, \sigma_i \rangle, \quad G_l^\mu = \langle G, \xi_l \rangle.$$

The k index refers to the Newton iteration. The form \mathcal{C}^μ depends on 3 different indexes and is assembled online for any given value of μ . Then for every k we have to incorporate in \mathcal{C}^μ the solution at the previous iteration to update the system matrix and the right-hand-side. We can adopt the following stopping criterium

$$\|\mathbf{u}_N^{(k+1)}(\mu) - \mathbf{u}_N^{(k)}(\mu)\| \leq \epsilon_N$$

where ϵ_N is a prescribed tolerance. When the Stokes solution is available, as in our case, it may be used as initial guess $\mathbf{u}_N^{(0)}$. If we compare the assembling and computational costs of Navier-Stokes reduced basis problem with respect to Stokes problem we have to increase by $O(KN^3)$ operations for the solution of the non-linear system (K is the number of Newton iterations). In fact we use more efficient and faster solvers with splitting procedures. The other computational cost comes from the assembling procedure of the matrix \underline{C} (advection term), whose theoretical assembling cost is $O(Q^c 8N^3)$. The assembling costs for \underline{A} , \underline{B} and \underline{F} are, respectively, $O(Q^a 4N^2)$, $O(Q^b 2N^2)$ and $O(N)$. The system (3.22) has the following block-structure:

$$\begin{pmatrix} \underline{A} + \underline{C}^{(k+1)} & \underline{B} \\ \underline{B}^T & 0 \end{pmatrix} \begin{pmatrix} \underline{\mathbf{u}}_N^{(k+1)} \\ \underline{p}_N^{(k+1)} \end{pmatrix} = \begin{pmatrix} \underline{F}^{(k)} \\ \underline{G} \end{pmatrix}. \quad (3.23)$$

Numerical results, which however refer only to cases with geometrical affine parametric dependence, will be reported in Section 6.

4 Parametrized formulation: non-affine parametric dependence

In this section we extend the previous formulation by considering a *non-affine mapping* from the true subdomains $\hat{\Omega}^r$ into the reference ones denoted with Ω^r .

For any $\hat{x} \in \hat{\Omega}^r$, $r = 1, \dots, R$, its image $x \in \Omega^r$ is now given by

$$x = T^r(\mu; \hat{x}), \quad 1 \leq r \leq R; \quad (4.24)$$

we thus write on Ω^r

$$\frac{\partial}{\partial \hat{x}_i} = \frac{\partial x_j}{\partial \hat{x}_i} \frac{\partial}{\partial x_j} = T_{ji}^r(\mu, x) \frac{\partial}{\partial x_j}. \quad (4.25)$$

Referring to problem (3.12) each elements in the system has the following form, for $1 \leq i, j \leq d$:

$$\begin{aligned} \mathcal{A}(\mu; \mathbf{u}, \mathbf{w}) &= \sum_{r=1}^R \int_{\Omega^r} \frac{\partial \mathbf{u}}{\partial x_i} \nu_{T_{ij}}^r(\mu, x) \frac{\partial \mathbf{w}}{\partial x_j} d\Omega \\ \mathcal{B}(\mu; p, \mathbf{w}) &= - \sum_{r=1}^R \int_{\Omega^r} p \chi_{T_{ij}}^r(\mu, x) \frac{\partial w_j}{\partial x_i} d\Omega \\ \mathcal{C}(\mu; \mathbf{u}, \mathbf{v}, \mathbf{w}) &= - \sum_{r=1}^R \int_{\Omega^r} u_i \pi_{T_{ij}}^r(\mu, x) \frac{\partial v_j}{\partial x_i} \mathbf{w} d\Omega \\ \langle F_s, \mathbf{w} \rangle &= \sum_{r=1}^R \int_{\Omega^r} \left(\hat{\mathbf{f}}^r |(T^r(\mu, x))^{-1}| \right) \mathbf{w} d\Omega. \end{aligned}$$

In Section 7 we report a test case and we show the explicit forms of the previous terms. The *transformation tensors* for *diffusion bilinear forms* with non-affine mappings are defined as follows:

$$\nu_{T_{ij}}^r(\mu, x) = T_{ii'}^r(\mu, x) \hat{\nu}_{i'j'} T_{jj'}^r(\mu, x) |(T^r(\mu, x))^{-1}|, \quad 1 \leq i, j \leq d, r = 1, \dots, R. \quad (4.26)$$

The tensors for *pressure*, *divergence* and *advection forms* are defined for non-affine mappings as:

$$\chi_{T_{ij}}^r(\mu, x) = \pi_{T_{ij}}^r(\mu, x) = T_{ij}^r(\mu, x) |(T^r(\mu, x))^{-1}|. \quad (4.27)$$

To decouple the non-affine contributions we apply the empirical interpolation procedure proposed in [1] to expand mapping terms and split the parameters dependent contribution from the one depending only on spacial coordinates. We can write:

$$\nu_{T_{ij}}^r(\mu, x) = \sum_{m=1}^{M_{ijr}^a} \beta_{ijm}^r(\mu) \gamma_{ijm}^r(x), \quad (4.28)$$

$$\chi_{T_{ij}}^r(\mu, x) = \pi_{T_{ij}}^r(\mu, x) = \sum_{m=1}^{M_{ijr}^b} \alpha_{ijm}^r(\mu) \omega_{ijm}^r(x), \quad (4.29)$$

where m refers to the interpolation functions we use for each form (related with the maximum interpolation error), i and j are indexes related to linear/bilinear

form, r refers to subdomains. β and α are weights depending on the parameters μ , while γ and ω are interpolation functions (“shape functions”) used as basis.

Let us recall the algorithm based on the empirical interpolation method proposed by Maday et al. in [1]:

$g(x, \mu)$, is the non – affine mapping term (i.e. a shape).

The goal is to expand

$$g_M(x, \mu) = \sum_{m=1}^M \beta_m(\mu) q_m(x), \quad (4.30)$$

as a sum of products decomposed in two parts: $\beta_m(\mu)$ are parameters dependent weights (computed many times for each value of μ); $q_m(x)$ are shape functions without a parametric dependence (computed only once).

The main elements are the test shape functions and the interpolation points, respectively:

$$W_M^g = \{\gamma_m = g(\cdot, \mu_m^g), 1 \leq m \leq M\}, \quad \text{with } \mu_m^g \text{ properly chosen,}$$

$$T_M = \{t_1, \dots, t_M\}, 1 \leq M \leq M_{max}, \text{ sets of interpolation points.}$$

The interpolation algorithm is:

$$\text{for } M = 1, \text{ set } t_1 = \text{argsup}_{x \in \Omega} |\gamma_1(x)|, \quad q_1 = \gamma_1(x) / \gamma_1(t_1), \text{ (off - line)}$$

$$\text{then, for } M = 2, \dots, M_{max} : \sum_{j=1}^{M-1} \sigma_j^{M-1} q_j(t_i) = \gamma_M(t_i), 1 \leq i \leq M-1, \text{ (off - line)}$$

$$r_M(x) = \gamma_M(x) - \sum_{j=1}^{M-1} \sigma_j^{M-1} q_j(x), t_M = \text{argsup}_{x \in \Omega} |r_M(x)|, \text{ (off - line)}$$

$$q_M(x) = r_M(x) / r_M(t_M); g_M(x, \mu) = \sum_{m=1}^M \beta_m(\mu) q_m(x), \text{ (off - line)}$$

$$\sum_{j=1}^M q_j(t_i) \beta_j(\mu) = g(t_i, \mu), 1 \leq i \leq M, \text{ (on - line).}$$

To stop the procedure we impose $\|g(\cdot, \mu) - g_M(\cdot, \mu)\|_{L^\infty(\Omega)} \leq \epsilon_{max}$ where ϵ_{max} is an interpolation error. We go back to our problem and, in order to build an *effectively affine* decomposition, we define:

$$\Psi^{t(i,j,r,m)}(\mu) = \beta_{ijm}^r(\mu), \quad \mathcal{A}^{t(i,j,r,m)}(\gamma(x), \mathbf{u}, \mathbf{w}) = \int_{\Omega^r} \gamma_{ijm}^r(x) \frac{\partial \mathbf{u}}{\partial x_i} \frac{\partial \mathbf{w}}{\partial x_j} d\Omega, \quad (4.31)$$

$$\Upsilon^{p(i,j,r,m)}(\mu) = \alpha_{ijm}^r(\mu), \quad \mathcal{B}^{p(i,j,r,m)}(\omega(x), p, \mathbf{w}) = - \int_{\Omega^r} \omega_{ijm}^r(x) p \frac{\partial w_i}{\partial x_j} d\Omega, \quad (4.32)$$

$$\Upsilon^{p(i,j,r,m)}(\mu) = \alpha_{ijm}^r(\mu), \quad \mathcal{C}^{p(i,j,r,m)}(\omega(x), \mathbf{u}, \mathbf{v}, \mathbf{w}) = - \int_{\Omega^r} \omega_{ijm}^r(x) u_j \frac{\partial v_i}{\partial x_j} \mathbf{w} d\Omega, \quad (4.33)$$

for $1 \leq r \leq R$, $1 \leq i, j \leq 2$, $1 \leq m \leq \max(M_{ijr}^a, M_{ijr}^b)$ (t and p are condensed indexes of i, j, r, m quantities). We rewrite our terms as:

$$\mathcal{A}(\mu, \mathbf{u}, \mathbf{w}) = \sum_{t=1}^{Q^a} \Psi^t(\mu) \mathcal{A}^t(\gamma(x), \mathbf{u}, \mathbf{w}),$$

$$\mathcal{B}(\mu, p, \mathbf{w}) = \sum_{p=1}^{Q^b} \Upsilon^p(\mu) \mathcal{B}^p(\omega(x), p, \mathbf{w}) ,$$

$$\mathcal{C}(\mu, \mathbf{u}, \mathbf{v}, \mathbf{w}) = \sum_{p=1}^{Q^c} \Upsilon^p(\mu) \mathcal{C}^p(\omega(x), \mathbf{u}, \mathbf{v}, \mathbf{w}) ,$$

in this case $Q^a = \sum_{j=1}^d \sum_{i=1}^d \sum_{r=1}^{R_T} M_{ijr}^a$; $Q^b = Q^c = \sum_{j=1}^d \sum_{i=1}^d \sum_{r=1}^{R_T} M_{ijr}^b$. We can now solve the Navier-Stokes problem written in (3.12) on the reference domain Ω for some snapshots values of parameter μ with the aim of building the reduced basis spaces. The formulation in this case is the same as the one in the previous section. We use the same supremizer option (the one with the μ^n off-line value) so that we have a reduced basis velocity space Y_N (3.17) which is μ independent. The only difference is the use of the *effectively affine dependence* of $\mathcal{B}(\mu; q, \mathbf{w})$ on the parameter which reads:

$$T^{\mu^n} \xi = \sum_{p=1}^{Q^b} \Upsilon^p(\mu^n) T^p \xi, \quad (4.34)$$

for any ξ and μ , where $T : Q_h \rightarrow Y_h$. We may write each T^p component of 4.34 as

$$(T^p \xi, \mathbf{w})_Y = \mathcal{B}^p(\omega, q, \mathbf{w}), \quad \forall \mathbf{w} \in Y_h.$$

Referring to the reduced basis non-linear system (3.22) we have the following sub-matrices A , B and C , respectively:

$$A_{ij}^\mu = \sum_{z=1}^{Q^a} \Psi^z(\mu) \mathcal{A}^z(\gamma, \sigma_i, \sigma_j), \quad 1 \leq i, j \leq 2N,$$

$$B_{il}^\mu = \sum_{z=1}^{Q^b} \Upsilon^z(\mu) \mathcal{B}^z(\omega, \sigma_i, \xi_l), \quad 1 \leq i \leq 2N, \quad 1 \leq l \leq N,$$

and

$$C_{ijh}^\mu = \sum_{z=1}^{Q^c} \Upsilon^z(\mu) \mathcal{C}^z(\omega, \sigma_i, \sigma_j, \sigma_h), \quad 1 \leq i, j, h \leq 2N.$$

Numerical results on the test case of a furrowed channel will be reported in Section 7.

5 Parametrized formulation: affine and non-affine combined parametric dependence

In this section we combine the formulations introduced in the two previous sections to allow for the application to parametrized domains with both affine (in

some subdomains) and non-affine (in the others) parametric dependence, as already done for the Stokes problem in [29]. In this case we use a different supremizer option, building reduced basis approximation space which is depending on the value of the “on-line” parameter μ . It is more complex and computationally expensive however it guarantees an “a-priori” stability of the method. We consider again the parametrized system of Navier-Stokes equations, whose formulation on the reference domain Ω is the following: find $(\mathbf{u}(\mu), p(\mu)) \in Y \times Q$:

$$\begin{cases} \mathcal{A}(\mu; \mathbf{u}(\mu), \mathbf{w}) + \mathcal{B}(\mu; p(\mu), \mathbf{w}) + \mathcal{C}(\mu; \mathbf{u}(\mu), \mathbf{u}(\mu), \mathbf{w}) = \langle F, \mathbf{w} \rangle \quad \forall \mathbf{w} \in Y, \\ \mathcal{B}(\mu; q, \mathbf{u}(\mu)) = \langle G^0, q \rangle \quad \forall q \in Q. \end{cases} \quad (5.35)$$

The problem has been traced back to a *reference domain* by an *affine mapping* on some subdomains $\hat{\Omega}_G^r$ into Ω_G^r and by a *non-affine mapping* on the remaining subdomains $\hat{\Omega}_T^r$ into Ω_T^r . More precisely, the physical domain $\hat{\Omega}$ is the union of two (finite) families of subdomains $\{\hat{\Omega}_G^r, r = 1, \dots, R_G\}$ and $\{\hat{\Omega}_T^r, r = 1, \dots, R_T\}$. Then $\hat{\Omega} = \text{int}(\bigcup_{r=1}^{R_G} \hat{\Omega}_G^r \cup \bigcup_{r=1}^{R_T} \hat{\Omega}_T^r)$. For any $\hat{x} \in \hat{\Omega}_G^r$, $r = 1, \dots, R_G$, its image $x \in \Omega_G^r$ is given by (3.10) and (3.11). On the other hand, for any $\hat{x} \in \hat{\Omega}_T^r$, $r = 1, \dots, R_T$, its image $x \in \Omega_T^r$ is given by (4.24) and (4.25). In the reference domain Ω we have:

$$\mathcal{A}(\mu; \mathbf{u}, \mathbf{w}) = \sum_{r=1}^{R_G} \int_{\Omega_G^r} \frac{\partial \mathbf{u}}{\partial x_i} \nu_{G_{ij}}^r(\mu) \frac{\partial \mathbf{w}}{\partial x_j} d\Omega + \quad (5.36)$$

$$\sum_{r=1}^{R_T} \int_{\Omega_T^r} \frac{\partial \mathbf{u}}{\partial x_i} \nu_{T_{ij}}^r(\mu, x) \frac{\partial \mathbf{w}}{\partial x_j} d\Omega$$

$$\mathcal{B}(\mu; p, \mathbf{w}) = - \sum_{r=1}^{R_G} \int_{\Omega_G^r} p \chi_{G_{ij}}^r(\mu) \frac{\partial w_j}{\partial x_i} d\Omega + \quad (5.37)$$

$$- \sum_{r=1}^{R_T} \int_{\Omega_T^r} p \chi_{T_{ij}}^r(\mu, x) \frac{\partial w_j}{\partial x_i} d\Omega$$

$$\mathcal{C}(\mu; \mathbf{u}, \mathbf{v}, \mathbf{w}) = \sum_{r=1}^{R_G} \int_{\Omega_G^r} u_i \pi_{G_{ij}}^r(\mu) \frac{\partial v_j}{\partial x_i} \mathbf{w} d\Omega + \quad (5.38)$$

$$- \sum_{r=1}^{R_T} \int_{\Omega_T^r} u_i \pi_{T_{ij}}^r(\mu, x) \frac{\partial v_j}{\partial x_i} \mathbf{w} d\Omega$$

$$\langle F, \mathbf{w} \rangle = \langle F_s, \mathbf{w} \rangle + \langle F^0, \mathbf{w} \rangle, \quad (5.39)$$

where

$$\langle F_s, \mathbf{w} \rangle = \sum_{r=1}^{R_G} \int_{\Omega_G^r} \left(\hat{\mathbf{f}}^r \det(G^r(\mu))^{-1} \right) \mathbf{w} d\Omega + \sum_{r=1}^{R_T} \int_{\Omega_T^r} \left(\hat{\mathbf{f}}^r \det(T^r(\mu, x))^{-1} \right) \mathbf{w} d\Omega, \quad (5.40)$$

$$\langle F^0, \mathbf{w} \rangle = -\langle \mathcal{A} \mathbf{g}_{in}, \mathbf{w} \rangle; \quad \langle G^0, q \rangle = \langle \mathcal{B} q, \mathbf{g}_{in} \rangle.$$

The *transformation tensors* for diffusion bilinear forms with affine and non-affine mappings are defined, respectively, as follows:

$$\nu_{G_{ij}}^r(\mu) = G_{ii'}^r(\mu) \hat{\nu}_{i'j'} G_{jj'}^r(\mu) \det(G^r(\mu))^{-1}, \quad 1 \leq i, j \leq d, r = 1, \dots, R_G, \quad (5.41)$$

$$\nu_{T_{ij}}^r(\mu, x) = T_{ii'}^r(\mu, x) \hat{\nu}_{i'j'} T_{jj'}^r(\mu, x) \det(T^r(\mu, x))^{-1}, \quad 1 \leq i, j \leq d, r = 1, \dots, R_T. \quad (5.42)$$

The tensors for *pressure, divergence and advection forms* are defined, respectively, for affine and non-affine mappings as:

$$\chi_{G_{ij}}^r(\mu) = \pi_{G_{ij}}^r(\mu) = G_{ij}^r \det(G^r(\mu))^{-1}, \quad (5.43)$$

$$\chi_{T_{ij}}^r(\mu, x) = \pi_{T_{ij}}^r(\mu, x) = T_{ij}^r(\mu, x) \det(T^r(\mu, x))^{-1}. \quad (5.44)$$

For the non-affine parts we apply, as already proposed, the empirical interpolation procedure to expand non-affine mapping terms and decouple the parameters dependent contribution from the one depending only on spacial coordinates. We write:

$$\nu_{T_{ij}}^r(\mu, x) = \sum_{m=1}^{M_{ijr}^a} \beta_{ijm}^r(\mu) \gamma_{ijm}^r(x), \quad (5.45)$$

$$\chi_{T_{ij}}^r(\mu, x) = \sum_{m=1}^{M_{ijr}^b} \alpha_{ijm}^r(\mu) \omega_{ijm}^r(x), \quad (5.46)$$

where m refers to the number of interpolation functions we use for each form (related with max interpolation error), i and j are indexes related to linear/bilinear form, r is the subdomain index, β and α are weighing quantities depending on the parameters μ , γ and ω are interpolation functions used as basis.

Furthermore, we define

$$\Theta^{q(i,j,r)}(\mu) = \nu_{G_{ij}}^r(\mu), \quad \mathcal{A}_G^{q(i,j,r)}(\mathbf{u}, \mathbf{w}) = \int_{\Omega_G^r} \frac{\partial \mathbf{u}}{\partial x_i} \frac{\partial \mathbf{w}}{\partial x_j} d\Omega, \quad (5.47)$$

$$\Phi^{s(i,j,r)}(\mu) = \chi_{G_{ij}}^r(\mu) = \pi_{G_{ij}}^r(\mu), \quad \mathcal{B}_G^{s(i,j,r)}(p, \mathbf{w}) = - \int_{\Omega_G^r} p \frac{\partial w_i}{\partial x_j} d\Omega, \quad (5.48)$$

$$\mathcal{C}_G^{s(i,j,r)}(\mathbf{u}, \mathbf{v}, \mathbf{w}) = \int_{\Omega_G^r} u_i \frac{\partial v_i}{\partial x_j} \mathbf{w} d\Omega, \quad (5.49)$$

for $1 \leq r \leq R_G$, $1 \leq i, j \leq d$ (q and s are condensed indexes of i, j, r quantities), and

$$\Psi^{t(i,j,r,m)}(\mu) = \beta_{ijm}^r(\mu), \quad \mathcal{A}_T^{t(i,j,r,m)}(\gamma(x), \mathbf{u}, \mathbf{w}) = \int_{\Omega_T^r} \gamma_{ijm}^r(x) \frac{\partial \mathbf{u}}{\partial x_i} \frac{\partial \mathbf{w}}{\partial x_j} d\Omega, \quad (5.50)$$

$$\Upsilon^{p(i,j,r,m)}(\mu) = \alpha_{ijm}^r(\mu), \quad \mathcal{B}_T^{p(i,j,r,m)}(\omega(x), p, \mathbf{w}) = - \int_{\Omega_T^r} \omega_{ijm}^r(x) p \frac{\partial w_i}{\partial x_j} d\Omega, \quad (5.51)$$

$$\mathcal{C}_T^{p(i,j,r,m)}(\omega(x), \mathbf{u}, \mathbf{v}, \mathbf{w}) = \int_{\Omega_T^r} \omega_{ijm}^r(x) u_i \frac{\partial v_i}{\partial x_j} \mathbf{w} d\Omega, \quad (5.52)$$

for $1 \leq r \leq R_T$, $1 \leq i, j \leq 2$, $1 \leq m \leq \max(M_{ijr}^a, M_{ijr}^b)$ (t and p are condensed indexes of i, j, r, m quantities used to simplify notation: each value of t or p represents a different combination of the previous four indexes i, j, r, m). We apply an *effectively affine* decomposition:

$$\begin{aligned} \mathcal{A}(\mu, \mathbf{u}, \mathbf{w}) &= \sum_{q=1}^{Q_G^a} \Theta^q(\mu) \mathcal{A}_G^q(\mathbf{u}, \mathbf{w}) + \sum_{t=1}^{Q_T^a} \Psi^t(\mu) \mathcal{A}_T^t(\gamma(x), \mathbf{u}, \mathbf{w}), \\ \mathcal{B}(\mu, p, \mathbf{w}) &= \sum_{s=1}^{Q_G^b} \Phi^s(\mu) \mathcal{B}_G^s(p, \mathbf{w}) + \sum_{p=1}^{Q_T^b} \Upsilon^p(\mu) \mathcal{B}_T^p(\omega(x), p, \mathbf{w}), \\ \mathcal{C}(\mu, \mathbf{u}, \mathbf{v}, \mathbf{w}) &= \sum_{s=1}^{Q_G^c} \Phi^s(\mu) \mathcal{C}_G^s(\mathbf{u}, \mathbf{v}, \mathbf{w}) + \sum_{p=1}^{Q_T^c} \Upsilon^p(\mu) \mathcal{C}_T^p(\omega(x), \mathbf{u}, \mathbf{v}, \mathbf{w}). \end{aligned}$$

If $\Omega \subset \mathbb{R}^d$, then $Q_G^a = d \times d \times d \times R_G$, $Q_G^b = d \times d \times R_G$, $Q_G^c = d \times d \times d \times R_G$; $Q_T^a = \sum_{j=1}^d \sum_{i=1}^d \sum_{r=1}^{R_T} M_{ijr}^a$; $Q_T^b = \sum_{j=1}^d \sum_{i=1}^d \sum_{r=1}^{R_T} M_{ijr}^b$ and $Q_T^c = \sum_{j=1}^d \sum_{i=1}^d \sum_{r=1}^{R_T} M_{ijr}^b$.

The non-linear problem (5.35) has to be discretized and then linearized to be solved, by an iterative method as seen in Section 3.

In the reduced basis approximation we choose properly (for instance by an optimization algorithm as proposed in [28]) a set of sample parameters $S_N^\mu = \{\mu^1, \dots, \mu^N\}$, where $\mu^n \in \mathcal{D}^\mu$, $n = 1, \dots, N$.

Correspondingly, we take a set of couples $(\mathbf{u}_h(\mu^n), p_h(\mu^n))$ which are approximate solutions of the Navier-Stokes problem (5.35) using the finite element method. Then the *reduced basis pressure space* is still taken as

$$Q_N = \text{span} \{ \xi_n, n = 1, \dots, N \}, \text{ where } \xi_n = p_h(\mu^n),$$

while for the *reduced basis velocity space* we take into consideration the option in which the space is μ dependent:

$$Y_N^\mu = \text{span} \{ \zeta_n, n = 1, \dots, N; T^\mu \xi_n, n = 1, \dots, N \}, \text{ where } \zeta_n = \mathbf{u}_h(\mu^n).$$

The reduced basis approximation problem reads: find $(\mathbf{u}_N(\mu), p_N(\mu)) \in Y_N \times Q_N$ s.t.:

$$\begin{cases} \mathcal{A}(\mu; \mathbf{u}_N(\mu), \mathbf{w}) + \mathcal{B}(\mu; p_N(\mu), \mathbf{w}) + \mathcal{C}(\mu; \mathbf{u}_N(\mu), \mathbf{u}_N(\mu), \mathbf{w}) = \langle F, \mathbf{w} \rangle \quad \forall \mathbf{w} \in Y_N, \\ \mathcal{B}(\mu; q, \mathbf{u}_N(\mu)) = \langle G^0, q \rangle \quad \forall q \in Q_N. \end{cases} \quad (5.53)$$

We rewrite for computational convenience Y_N^μ using the *effectively affine dependence* of $\mathcal{B}(\mu; q, \mathbf{w})$ on the parameter and the *linearity* of T^μ :

$$T^\mu \xi = \sum_{q=1}^{Q_G^b} \Phi^q(\mu) T_G^q \xi + \sum_{p=1}^{Q_T^b} \Upsilon^p(\mu) T_T^p \xi \quad (5.54)$$

for any ξ and μ , where:

$$\begin{aligned}(T_G^q \xi, \mathbf{w})_Y &= \mathcal{B}_G^q(q, \mathbf{w}) \quad \forall \mathbf{w} \in Y_h, \\ (T_T^p \xi, \mathbf{w})_Y &= \mathcal{B}_T^p(\omega, q, \mathbf{w}) \quad \forall \mathbf{w} \in Y_h,\end{aligned}$$

which allows us to write:

$$Y_N^\mu = \text{span} \left\{ \sum_{k=1}^{\overline{Q}_G^b} \Phi^k(\mu) \sigma_{kn} + \sum_{k'=1}^{Q_T^b} \Upsilon^{k'}(\mu) \tilde{\sigma}_{k'n}, n = 1, \dots, 2N \right\},$$

where $\overline{Q}_G^b = Q_G^b + 1, \Phi^{\overline{Q}_G^b} = 1$.

For $n = 1, \dots, N$:

$$\begin{aligned}\sigma_{kn} &= 0, \text{ for } k = 1, \dots, Q_G^b; \\ \tilde{\sigma}_{k'n} &= 0, \text{ for } k' = 1, \dots, Q_T^b; \\ \sigma_{\overline{Q}_G^b n} &= \zeta_n = \mathbf{u}_h(\mu^n).\end{aligned}$$

For $n = N + 1, \dots, 2N$:

$$(\sigma_{kn}, \mathbf{w})_Y = \mathcal{B}_G^k(\xi_{n-N}, \mathbf{w}), \forall \mathbf{w} \in Y_h, \text{ for } k = 1, \dots, Q_G^b; \quad (5.55)$$

$$\sigma_{\overline{Q}_G^b n} = 0;$$

$$(\tilde{\sigma}_{kn}, \mathbf{w})_Y = \mathcal{B}_T^k(\omega, \xi_{n-N}, \mathbf{w}), \forall \mathbf{w} \in Y_h, \text{ for } k = 1, \dots, Q_T^b. \quad (5.56)$$

For a new value of the parameter μ we look for a solution given by a combination of previously computed stored solutions as basis functions, i.e.:

$$\begin{aligned}\mathbf{u}_N(\mu) &= \sum_{j=1}^{2N} u_{Nj}(\mu) \left(\sum_{k=1}^{\overline{Q}_G^b} \Phi^k(\mu) \sigma_{kj} + \sum_{k'=1}^{Q_T^b} \Upsilon^{k'}(\mu) \tilde{\sigma}_{k'j} \right), \\ p_N(\mu) &= \sum_{l=1}^N p_{Nl}(\mu) \xi_l,\end{aligned}$$

whose unknowns u_{Nj} and p_{Nl} satisfy the following non-linear system:

$$\begin{cases} \sum_{j=1}^{2N} A_{ij}^\mu \mathbf{u}_{Nj}(\mu) + \sum_{l=1}^N B_{il}^\mu p_{Nl}(\mu) + \sum_{h=1}^{2N} \sum_{j=1}^{2N} \mathbf{u}_{Nh}(\mu) C_{ijh}^\mu \mathbf{u}_{Nj}(\mu) = F_i, & 1 \leq i \leq 2N, \\ \sum_{j=1}^{2N} B_{jl}^\mu \mathbf{u}_{Nj}(\mu) = G_l, & 1 \leq l \leq N. \end{cases} \quad (5.57)$$

To solve it we apply the Newton method which yields the following iteration:

for $k \geq 0$ given $\mathbf{u}_{Nj}^{(k)}$, find $\mathbf{u}_{Nj}^{(k+1)}$ and $p_{Nl}^{(k+1)}$ such that

$$\begin{cases} \sum_{j=1}^{2N} A_{ij}^\mu \mathbf{u}_{Nj}^{(k+1)}(\mu) + \sum_{l=1}^N B_{il}^\mu p_{Nl}^{(k+1)}(\mu) + \sum_{h=1}^{2N} \sum_{j=1}^{2N} \mathbf{u}_{Nh}^{(k)}(\mu) C_{ijh}^\mu \mathbf{u}_{Nj}^{(k+1)}(\mu) + \\ + \sum_{h=1}^{2N} \sum_{j=1}^{2N} \mathbf{u}_{Nh}^{(k+1)}(\mu) C_{ijh}^\mu \mathbf{u}_{Nj}^{(k)}(\mu) = F_i^\mu + \sum_{h=1}^{2N} \sum_{j=1}^{2N} \mathbf{u}_{Nj}^{(k)}(\mu) C_{ijh}^\mu \mathbf{u}_{Nh}^{(k)}(\mu) \\ \sum_{j=1}^{2N} B_{jl}^\mu \mathbf{u}_{Nj}^{(k+1)}(\mu) = G_l^\mu, & 1 \leq l \leq N, \quad 1 \leq i \leq 2N. \end{cases} \quad (5.58)$$

The sub-matrices A , B and C are given by:

$$\begin{aligned}
A_{ij}^\mu &= \sum_{z=1}^{Q_G^a} \sum_{k'=1}^{\bar{Q}_G^b} \sum_{k''=1}^{\bar{Q}_G^b} \Theta^z(\mu) \Phi^{k'}(\mu) \Phi^{k''}(\mu) \mathcal{A}_G^z(\sigma_{k'i}, \sigma_{k''j}) + \\
&+ \sum_{z=1}^{Q_T^a} \sum_{k'=1}^{Q_T^b} \sum_{k''=1}^{Q_T^b} \Psi^z(\mu) \Upsilon^{k'}(\mu) \Upsilon^{k''}(\mu) \mathcal{A}_T^z(\gamma, \tilde{\sigma}_{k'i}, \tilde{\sigma}_{k''j}), \quad 1 \leq i, j \leq 2N; \\
B_{il}^\mu &= \sum_{z=1}^{\bar{Q}_G^b} \sum_{k'=1}^{Q_G^b} \Phi^z(\mu) \Phi^{k'}(\mu) \mathcal{B}_G^z(\sigma_{k'i}, \xi_l) + \\
&+ \sum_{z=1}^{Q_T^b} \sum_{k'=1}^{Q_T^b} \Upsilon^z(\mu) \Upsilon^{k'}(\mu) \mathcal{B}_T^z(\omega, \tilde{\sigma}_{k'i}, \xi_l), \quad 1 \leq i \leq 2N, \quad 1 \leq l \leq N; \\
C_{ijh}^\mu &= \sum_{z=1}^{Q_G^c} \sum_{k'=1}^{\bar{Q}_G^b} \sum_{k''=1}^{\bar{Q}_G^b} \sum_{k'''=1}^{\bar{Q}_G^b} \Phi^z(\mu) \Phi^{k'}(\mu) \Phi^{k''}(\mu) \Phi^{k'''}(\mu) \mathcal{C}_G^z(\sigma_{k'i}, \sigma_{k''j}, \sigma_{k'''h}) + \\
&+ \sum_{z=1}^{\bar{Q}_T^c} \sum_{k'=1}^{Q_T^b} \sum_{k''=1}^{Q_T^b} \sum_{k'''=1}^{Q_T^b} \Upsilon^z(\mu) \Upsilon^{k'}(\mu) \Upsilon^{k''}(\mu) \Upsilon^{k'''}(\mu) \mathcal{C}_T^z(\omega, \tilde{\sigma}_{k'i}, \tilde{\sigma}_{k''j}, \tilde{\sigma}_{k'''h}), \quad 1 \leq i, j, h \leq 2N; \\
F_i &= \sum_{k'=1}^{\bar{Q}_G^b} \Phi^{k'}(\mu) \langle F, \sigma_{k'i} \rangle + \sum_{k'=1}^{Q_T^b} \Upsilon^{k'}(\mu) \langle F, \tilde{\sigma}_{k'i} \rangle, \quad 1 \leq i \leq 2N; \\
G_l &= \langle G^0, \xi_l \rangle, \quad 1 \leq l \leq N.
\end{aligned}$$

In compact form the linearized problem (5.58) can therefore be written as:

$$\begin{pmatrix} \underline{A} + \underline{C}^{(k+1)} & \underline{B} \\ \underline{B}^T & \underline{0} \end{pmatrix} \begin{pmatrix} \underline{\mathbf{u}}_N^{(k+1)} \\ \underline{\mathbf{p}}_N^{(k+1)} \end{pmatrix} = \begin{pmatrix} \underline{F}^{(k)} \\ \underline{G} \end{pmatrix}. \quad (5.59)$$

This reduced basis formulation is more involved than the one introduced in Section 4 due to (i) the coupling between affine and non-affine maps in different subdomains, (ii) the use of a different supremizer which is μ dependent, yielding a different reduced basis velocity approximation space. This results in an increased on-line complexity. By accounting also for the computation of supremizer components in the velocity space the following number of operations is needed in order to build reduced basis matrices: $O(Q^a(\bar{Q}^b)^2 4N^2)$ for sub-matrix \underline{A} , $O((\bar{Q}^b)^2 2N^2)$ for \underline{B} , $O(Q^c(\bar{Q}^b)^3 8N^3)$ for \underline{C} , $O(\bar{Q}^b N)$ for \underline{F} and $O(N^3)$ for the “inversion” of the full reduced basis matrix (5.59) at each Newton iteration, where $Q^a = Q_T^a + Q_G^a$, $\bar{Q}^b = \bar{Q}_G^b + Q_T^b$, $Q^c = Q_G^c + Q_T^c$. The quantities Q_G^a , Q_G^b and Q_G^c are depending only on the number of subdomains with affine

mappings (R_G), while quantities Q_T^a , Q_T^b and Q_T^c are depending also on the number of “shape functions” ($\gamma(x)$ and $\omega(x)$) related with interpolation error (ε_{max}) and the number of subdomains with non-affine mappings (R_T).

Some numerical results obtained by the reduced basis approximation introduced in this section will be reported in Section 8.

6 Some preliminary results: a simple channel

For our first test on the use of reduced basis for Navier-Stokes equations we deal only with affine mapping on a rectangular domain ($R = 1$, $d = 2$), parametrized by two quantities D and t , see Figure 1 (right). The parameters range is: $0.1 \leq D \leq 1.5$ and $0.1 \leq t \leq 1.5$.

To solve the parametrized Navier-Stokes problem in the domain outlined in Figure 1 we have imposed zero Dirichlet conditions on the boundary Γ_D , Neumann homogeneous conditions on the inflow Γ_{Ni} and outflow Γ_{No} : $\tau = (\nu \frac{\partial \mathbf{u}}{\partial \hat{\mathbf{n}}} - p \hat{\mathbf{n}}) = 0$, with $\hat{\mathbf{n}}$ normal unit vector.

We have considered a forcing term $\mathbf{f} = 10 \cdot (x, y)^T$ in order to create a flow acceleration, to have a non-zero velocity in y -direction and not only a parabolic velocity profile. Using the compact notation of Section 3 (3.13 and 3.14) and transformation (3.11) we get the following tensor for diffusion, divergence and transport forms, respectively:

$$\nu = \tilde{\nu} \begin{bmatrix} \frac{t}{D} & 0 \\ 0 & \frac{D}{t} \end{bmatrix}, \chi = \pi = \begin{bmatrix} t & 0 \\ 0 & D \end{bmatrix},$$

where $\tilde{\nu} = 0.04 N s m^{-2}$ is the viscosity.

Taylor-Hood finite elements, i.e. \mathbb{P}^2 elements for velocity (with supremizer) and \mathbb{P}^1 for pressure, have been used to build offline approximation basis functions [21]. The problem has been solved using the *pressure-matrix method*. The average *Reynolds* number considered was of order 10^2 (a low Reynolds number). Changing the parameter D (channel diameter) yields a variation of the Reynolds number.

At this step we have applied the reduced basis method and assembled the approximation spaces as described in Section 3. The basis is assembled as in Figure 1 (left) where we report the value of D and t , corresponding to each $\mathbf{u}_h(\mu)$ solution used as basis function increasing N and where $\mu = (D, t)$.

Figure 2 shows numerical results (mean and max H^1 and L^2 relative errors on velocity and pressure, respectively, on a large number of configurations) at different N . The reduced basis solutions have been compared directly with the approximate finite element solutions: the associated H^1 relative error for velocity and L^2 relative error for pressure are computed.

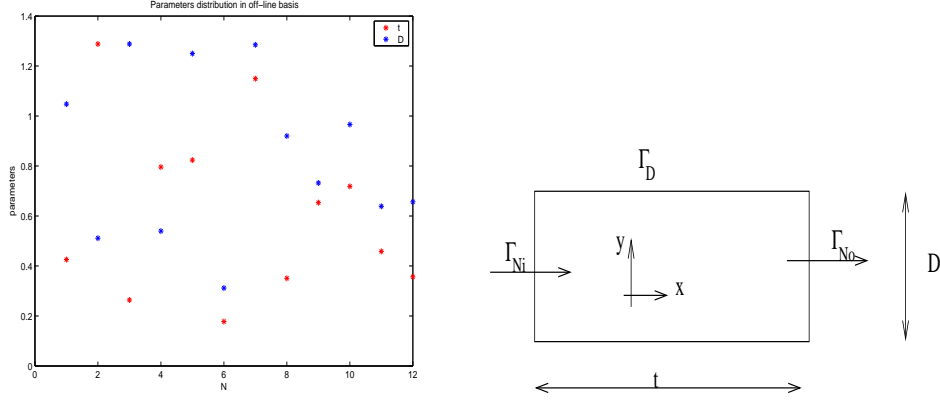


Figure 1: Parameters (D, t) distribution during basis assembling (left) and the simple domain configuration considered (right).

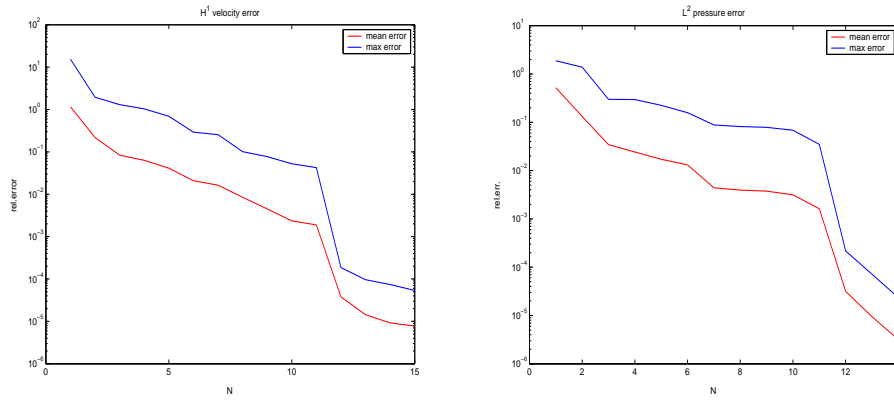


Figure 2: H^1 and L^2 relative errors on velocity and pressure, first test with 2 varying parameters (D, t) .

7 Furrowed channel test

Our second test deals with non-affine mapping on a rectangular domain ($R = 1$), considering a channel with an upper wall parametrized by a sinusoidal law, see Figure 3 (left). This may be regarded as a simplified stenotic arterial flow, that was already investigated e.g. by Sobey and Stephanoff [31] and [32]. We have used the formulation introduced in Section 4. We briefly recall the assumptions that we have made during this study. To solve the parametrized Navier-Stokes problem in the domain outlined in Figure 3 we have imposed zero Dirichlet conditions on the boundary Γ_D , Neumann non-homogeneous conditions on the inflow Γ_{Ni} ($\tau_{\hat{\mathbf{n}}} = 1, \tau_{\hat{\mathbf{t}}} = 0$, where $\tau = (\nu \frac{\partial \mathbf{u}}{\partial \hat{\mathbf{n}}} - p \hat{\mathbf{n}})$, with $\hat{\mathbf{n}}$ and $\hat{\mathbf{t}}$ normal and tangential directions, respectively) and Neumann homogeneous conditions on outflow Γ_{No} ($\tau_{\hat{\mathbf{n}}} = 0, \tau_{\hat{\mathbf{t}}} = 0$).

We consider one parameter μ ranging in $[-0.8, 0.8]$ to describe the upper arterial wall in the physical domain, through $\hat{x}_2 = f(\hat{x}_1, \mu) = 1 + \mu \sin(2\pi\hat{x}_1)$ (we have a single domain subject to a unique non-affine mapping). Figures 3-5 show some simulations to better describe the fluid dynamics phenomena involved in this case of study. The upper curved wall is responsible of the variation of the channel section and thus of the velocity gradient. Interesting phenomena to be “captured” by reduced basis method are the vertical velocity behavior (see Figure 5 on the right) and the development of a secondary flow (to be superimposed to the mainstream channel) when $|\mu|$ increases (see Figure 4 on the right). In Sobey [31] an accurate study of both steady and unsteady flows has been carried out dealing with furrowed channels at different Reynolds number, in particular focusing the attention over the secondary flows in the hollow zone of the channel. In our case the Reynolds number ranges between 10^2 and $4 \cdot 10^3$.

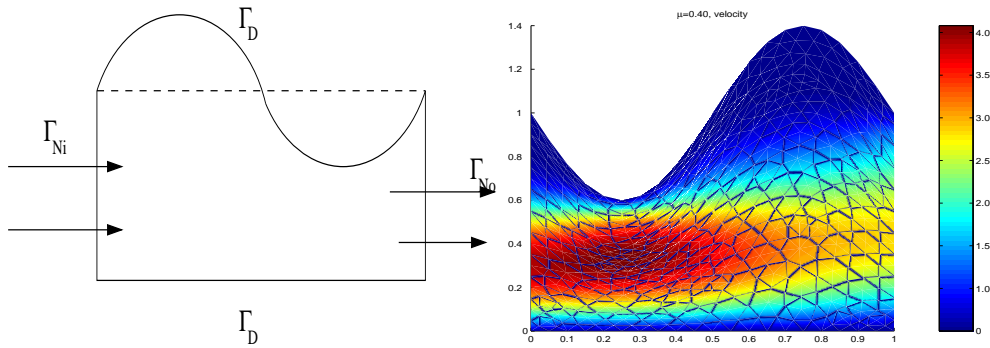


Figure 3: Portion of the geometrical domain for curved wall test model problem at $\mu = -0.4$ (left) and velocity (absolute value) for $\mu = 0.4$, $Re = 100$ (right).

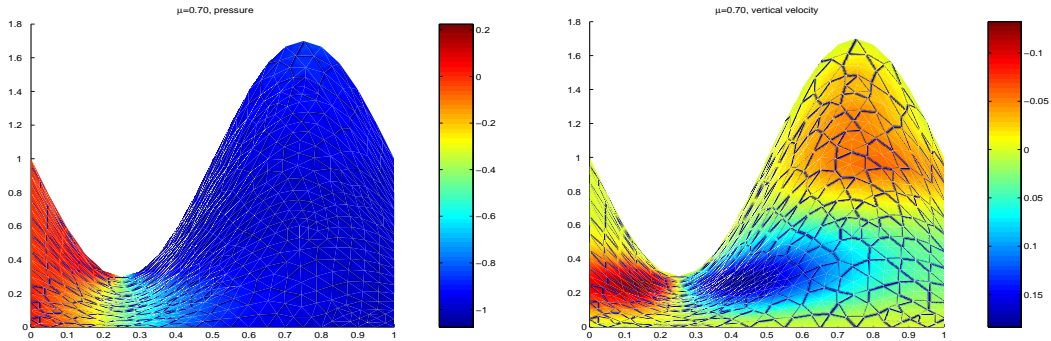


Figure 4: Values of pressure (left) and values of vertical velocity (right), for $\mu = 0.7$ and $Re = 100$.

Referring to Section 4 we have $\Omega_G = \emptyset$ and $\Omega_T = \Omega$, so $R_T = 1$.

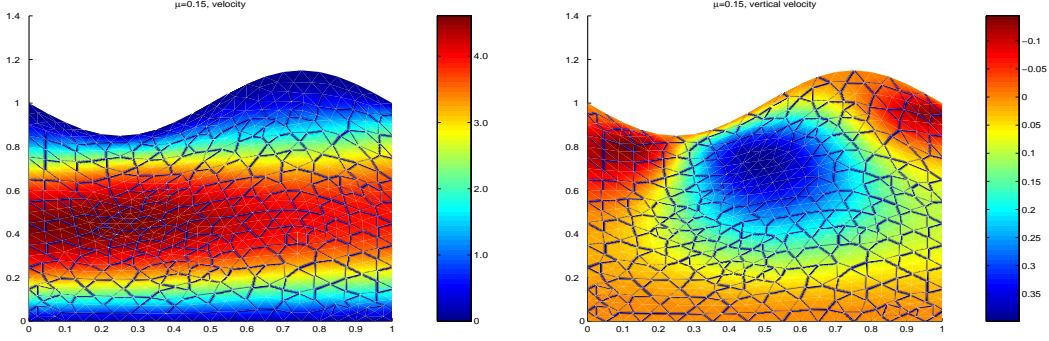


Figure 5: Absolute value of velocity (left) and values of vertical velocity (right), for $\mu = 0.15$ and $Re = 100$.

The coordinate transformation is $\mathcal{T} : \hat{\Omega} \rightarrow \Omega$, $\mathbf{x} = \mathcal{T}(\hat{\mathbf{x}})$, with

$$(x_1, x_2) = \mathcal{T}(\hat{x}_1, \hat{x}_2) = \left(\hat{x}_1, \frac{1}{f(\hat{x}_1, \mu)} \hat{x}_2 \right) \quad (7.60)$$

in Ω . Then,

$$d\hat{x}_1 d\hat{x}_2 = f(x_1, \mu) dx_1 dx_2,$$

and the following relations hold (with $f_{x_1} := \frac{df}{dx_1}$):

$$\begin{cases} \frac{\partial \hat{\mathbf{u}}}{\partial \hat{x}_2} = \frac{1}{f(x_1, \mu)} \frac{\partial \mathbf{u}}{\partial x_2}, \\ \frac{\partial \hat{\mathbf{u}}}{\partial \hat{x}_1} = \frac{\partial \phi}{\partial x_1} - x_2 \frac{f_{x_1}(x_1, \mu)}{f(x_1, \mu)} \frac{\partial \mathbf{u}}{\partial x_2}. \end{cases} \quad (7.61)$$

$$\nabla \cdot \hat{\mathbf{u}} = \frac{\partial u_1}{\partial x_1} - x_2 \frac{f_{x_1}(x_1, \mu)}{f(x_1, \mu)} \frac{\partial u_1}{\partial x_2} + \frac{1}{f(x_1, \mu)} \frac{\partial u_2}{\partial x_2}. \quad (7.62)$$

Using the compact notation (4.26) and (4.27) and transformation (7.60) we get the following tensor for diffusion and divergence (and advection) forms, respectively:

$$\nu_T = \nu \begin{bmatrix} f(x_1, \mu) & -f'_{x_1}(x_1, \mu)x_2 \\ -f'_{x_1}(x_1, \mu)x_2 & \frac{1}{f(x_1, \mu)} + \frac{f'^2_{x_1}(x_1, \mu)}{f(x_1, \mu)}x_2^2 \end{bmatrix}, \quad (7.63)$$

$$\chi_T = \pi_T = \begin{bmatrix} f(x_1, \mu) & -f'_{x_1}(x_1, \mu)x_2 \\ 0 & 1 \end{bmatrix}, \quad (7.64)$$

where ν is the viscosity [Nsm^{-2}] whose value was varied in simulating flows at different Reynolds number. Referring to (4.30) we get 5 different coefficient functions $g_M^j(x, \mu)$ to expand.

We apply empirical interpolation (4.28) and (4.29) to the tensors (7.63) and (7.64) and we impose a maximum interpolation error ε_{max} , thus considering different M_{max} “shape functions” for each $g_M^j(x, \mu)$. Each $g_M^j(x, \mu)$ represents a different coefficient for a different term of our problem ($j = 5$ in this test case).

Owing to empirical interpolation we expand each tensor component to apply an effectively affine decomposition:

$$\nu_T = \nu \begin{bmatrix} \sum_{m=1}^{M_{11}^a} \beta_{11m}(\mu) \gamma_{11m}(x) & \sum_{m=1}^{M_{12}^a} \beta_{12m}(\mu) \gamma_{12m}(x) \\ \sum_{m=1}^{M_{21}^a} \beta_{21m}(\mu) \gamma_{21m}(x) & \sum_{m=1}^{M_{22}^a} \beta_{22m}(\mu) \gamma_{22m}(x) \end{bmatrix}.$$

Note that this tensor is symmetric. Moreover,

$$\chi_T = \pi_T = \begin{bmatrix} \sum_{m=1}^{M_{11}^b} \alpha_{11m}(\mu) \omega_{11m}(x) & \sum_{m=1}^{M_{12}^b} \alpha_{12m}(\mu) \omega_{12m}(x) \\ 0 & 1 \end{bmatrix}.$$

The subdomain index r is omitted (in this case $R = 1$).

At this step we may apply the reduced basis formulation to this case and assemble the approximation spaces Y_N (3.17) and Q_N (3.16).

7.1 Results for low Reynolds number

We report some numerical results dealing with the solution of the furrowed channel rebuilt by reduced basis method. First we consider low Reynolds number (~ 100). Figures 6 and 7 show convergence results (mean and maximum H^1 and L^2 relative errors on velocity and pressure, respectively, testing a large number of configurations) at different N and for different values of maximum interpolation error ε_{max} . At the end of the test we have carried out also a comparison between empirical interpolation (using $g_M^j(x, \mu)$) and true functions ($g^j(x, \mu)$). We can see that for $\varepsilon_{max} \leq 10^{-8}$ we have accurate results that are not dominated or affected by interpolation error. When the interpolation error is dominating, the reduced basis error is characterized by a constant “plateau” and is not diminished by increasing N (see for example the case in which $\varepsilon_{max} \geq 10^{-6}$).

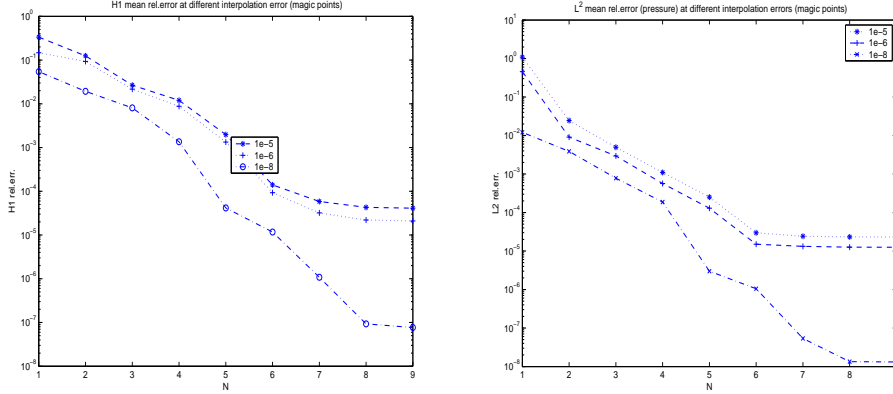


Figure 6: H^1 and L^2 relative mean error on velocity and pressure ($\nu = 0.1$) at different ε_{max} imposed on all $g_M^j(x, \mu)$ (a large number of testing configurations).

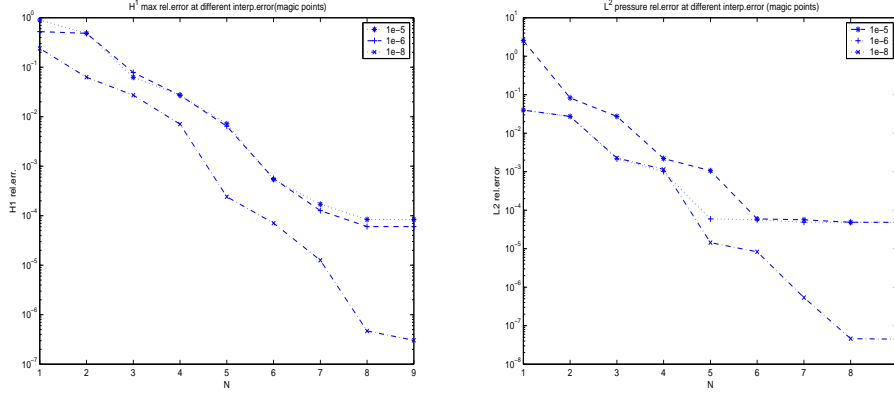


Figure 7: H^1 and L^2 relative max error on velocity and pressure ($\nu = 0.1$) at different ϵ_{max} imposed on all $g_M^j(x, \mu)$ (a large number of testing configuration).

7.2 Results for moderate Reynolds number

A further test case is concerned with moderate Reynolds number ($\sim 4 \cdot 10^3$). We have reported in Figure 8 convergence results using a max interpolation error $\epsilon_{max} \leq 10^{-6}$. The comparison is always made between the “true” approximated solution by finite element method and the “interpolated” one by reduced basis.

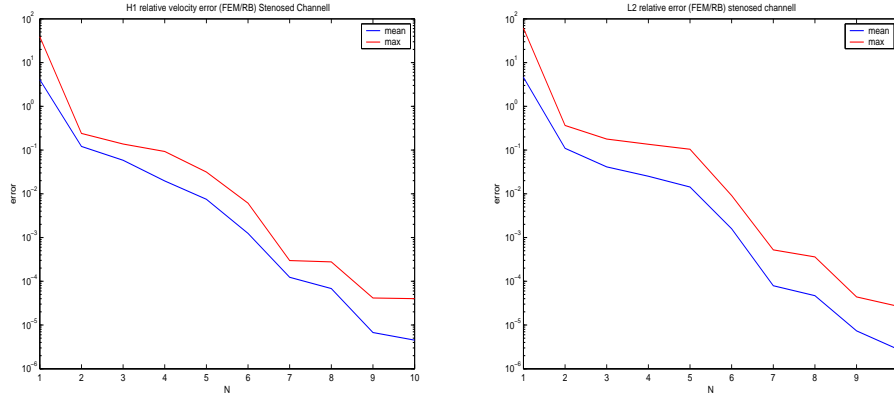


Figure 8: H^1 and L^2 relative error (max and mean) on velocity and pressure ($\nu = 0.04$) (testing a great number of configurations).

7.3 Reduced basis computational costs

At the end of this section we make some comments on the computational costs when using the reduced basis in the on-line stage at different Reynolds number. This completes the framework related with assembling and computational costs. For simplicity we consider the case of the problem of the furrowed channel with

one varying parameter and at different Reynolds number (at different viscosity values). Figure 9 shows on-line reduced basis computational cost (cputime on a IBM®T42 ThinkPad with a processor Pentium M 1.80 GHz and 1.0 Gb of Ram) for increasing N , compared with the computational cost of a finite element numerical simulation; the Reynolds number is $Re \leq 400$. We can see that reduced basis computational costs are $\sim 20\%$ of the finite element off-line solutions if we choose $N = 12$ corresponding to an H^1 error on velocity of $O(10^{-6})$, as shown in the picture on the right. The reduced basis approximation spaces have been optimized during the assembling procedures [28]. When increasing the Reynolds number ($400 \leq Re \leq 4000$) the computational saving of reduced basis techniques are at least of two orders of magnitude (i.e 1%) as shown in Figure 10, where on the right we have also a zoom representing online computational cost when increasing N . Results in fact depend on the choice of the initial guess for Newton iterations: in our case we have used Stokes solution (easily calculated and stored). Other elements influencing computational costs are the setting of the tolerance for the Newton algorithm (difference between the solutions of two successive iterations), in our case set to 10^{-8} . The numerical approximation of steady Navier-Stokes equations has been carried out by using a parametrized version of *MLife*, a FEM library (developed by F. Saleri at MOX) in Matlab-PDE toolbox environment where we have considered $\mathbb{P}^2 - \mathbb{P}^1$ elements for velocity and pressure, respectively, over a triangulation of $O(10^4)$ elements (see also Gresho and Sani [9]). The sparse linear system has been solved using *pressure-matrix method* (which is a block LU type decomposition of the system matrix) to compute velocity in two steps and to decouple the calculation of pressure from velocity (see [21]). The iterative methods used to solve the linearized system at each iteration have been *GMRES* and *Bi-CGSTAB* [22]. To improve computational efficiency we have used the *Cahouet-Chabard preconditioner*, see [4].

We observe that the use of reduced basis is providing real-time solutions (or related outputs) of a non-linear parametrized problems, whose solution would be quite expensive even if considering efficient FEM solvers. The importance of real-time accurate solutions increases when considering optimization problems involving also non-affine geometrical parametric dependence, as seen in the example of the furrowed channel.

8 The bypass problem

As last example, we consider a parametrized arterial bypass, as represented in Figure 11 the configuration is represented in terms of the vector of parameters $\mu = \{t, D, L, S, H, \theta, v\} \in \mathcal{D}^\mu \subset \mathbb{R}^P$ with \mathcal{D}^μ given by:

$[t_{min}, t_{max}] \times [D_{min}, D_{max}] \times [L_{min}, L_{max}] \times [S_{min}, S_{max}] \times [H_{min}, H_{max}] \times [\theta_{min}, \theta_{max}] \times [v_{min}, v_{max}]$. This test problem features both affine and non-affine parameters dependence in different subdomains and it represents an application of the for-

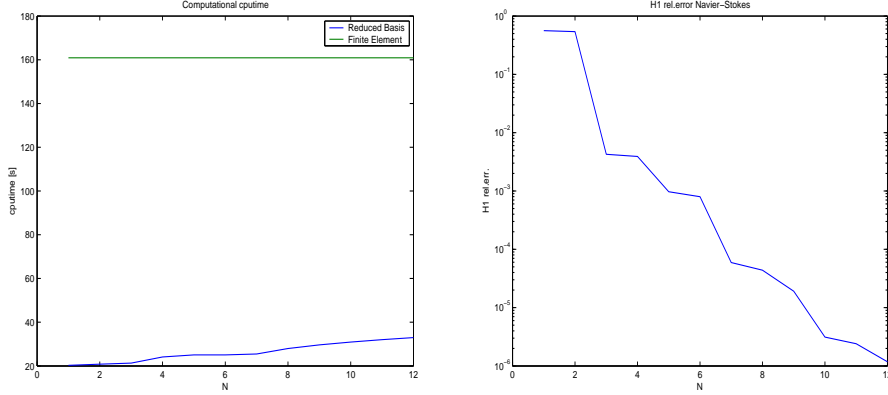


Figure 9: Online average computational costs of reduced basis in comparison with finite element simulation (left) and H^1 reduced basis velocity error increasing N (right) for channel flow at low Reynolds numbers.

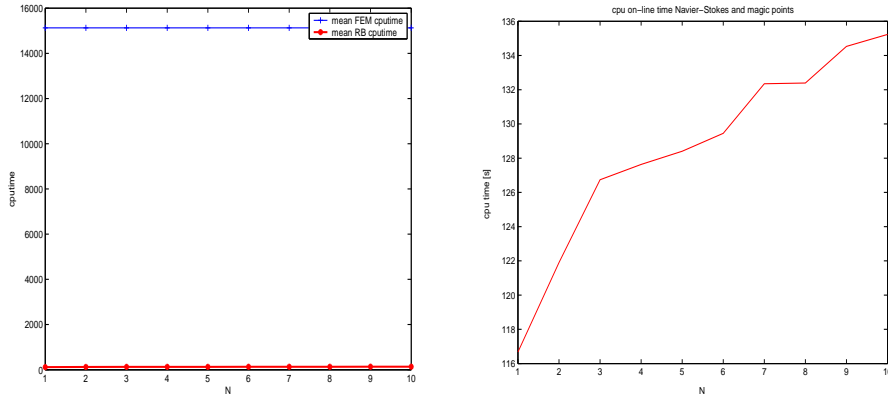


Figure 10: Online average computational costs of reduced basis for channel flow at higher Reynolds numbers.

mulation introduced in Section 5. The aim of this test is to combine the study of affine and non-affine terms in the same non-linear problem by varying different geometrical parameters and then to test the convergence of the reduced basis approximation, to extract output information and to carry out a sensitivity analysis on parameters. Referring to notation in Section 5 we have $R_G = 3$ (number of subdomains with affine dependence, precisely $\Omega^2, \Omega^3, \Omega^4$), $R_T = 1$ (number of subdomains with non-affine dependence, i.e Ω^1). The coordinate transformation in Ω^1 with non-affine parameter dependence is given by:

$$\begin{cases} x_1 = \frac{1}{H} \hat{x}_1 \\ x_2 = \frac{1}{l} (\hat{x}_2 - (vH^2 x_1 (x_1 - 1) + Hx_1 \tan(\theta))). \end{cases} \quad (8.65)$$

The role of parameters t and H is to stretch subdomain Ω^1 (as L, S, D stretch the remaining subdomains), the parameter v introduces a curvature in the walls of the incoming branch of the bypass and θ is responsible for a rigid rotation by letting the graft angle vary. The tensors for *viscous bilinear terms* are given by:

$$\nu_T^1 = \nu \begin{bmatrix} \frac{t}{H} & -(\tan \theta + 2vHx_1 - vH) \\ -(\tan \theta + 2vHx_1 - vH) & \frac{(1+(\tan \theta + 2vHx_1 - vH)^2)}{t} H \end{bmatrix}; \quad (8.66)$$

$$\nu_G^2 = \nu \begin{bmatrix} \frac{S}{D} & 0 \\ 0 & \frac{D}{S} \end{bmatrix}; \nu_G^3 = \nu \begin{bmatrix} \frac{t}{D} & 0 \\ 0 & \frac{D}{t} \end{bmatrix}; \nu_G^4 = \nu \begin{bmatrix} \frac{L}{D} & 0 \\ 0 & \frac{D}{L} \end{bmatrix}. \quad (8.67)$$

The tensors for *pressure, divergence and transport terms* are given by:

$$\chi_T^1 = \pi_T^1 = \begin{bmatrix} t & -H(\tan \theta + 2vHx_1 - vH) \\ 0 & H \end{bmatrix}; \chi_G^2 = \pi_G^2 = \begin{bmatrix} S & 0 \\ 0 & D \end{bmatrix}; \quad (8.68)$$

$$\chi_G^3 = \pi_G^3 = \begin{bmatrix} t & 0 \\ 0 & D \end{bmatrix}; \chi_G^4 = \pi_G^4 = \begin{bmatrix} L & 0 \\ 0 & D \end{bmatrix}. \quad (8.69)$$

We apply empirical interpolation expansion to the components of tensors ν_T^1, χ_T^1 and π_T^1 and we build the reduced basis approximation spaces for velocity and pressure.

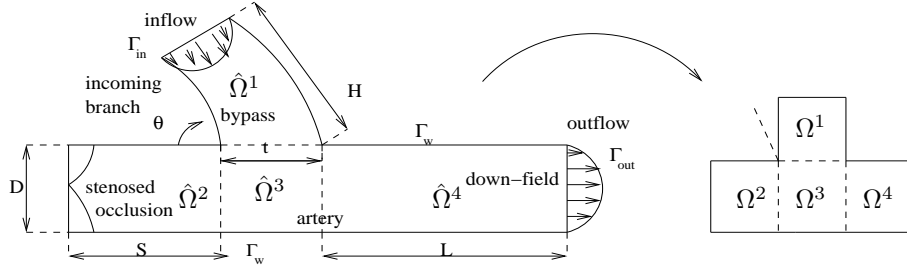


Figure 11: Geometrical scheme for the bypass test problem (physical domain at left and reference domain at right).

We have carried out some tests based on the same geometry considering five different varying parameters (we have frozen L and H). In particular we are interested in varying graft angle θ and curvature v (defining the upstream geometry) and the ratio $\frac{t}{D}$. In Figures 12 and 13 we report numerical results (max and mean H^1 errors on velocity and L^2 errors for pressure) considering several configurations at different N for two different maximum interpolation error $\varepsilon_{max} = 10^{-5}$ and then $\varepsilon_{max} = 10^{-8}$; these strict tolerances prevent interpolation error to overwhelm our approximation with the constant “plateau” in error plots.

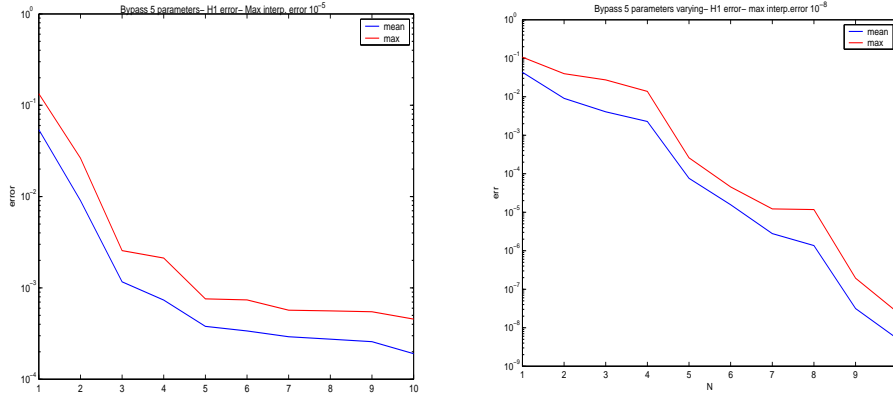


Figure 12: H^1 relative errors on velocity with different ϵ_{max} interpolation error imposed on all $g_M^j(x, \mu)$ (testing hundreds of different configurations with 5 different parameters varying).

8.1 Outputs sensitivities

We conclude this section with two different studies on the bypass problem providing a comparison between Stokes and Navier-Stokes solutions (and outputs of interest) and some considerations about the influence of curvature of the upper stream geometry. The ratio $\frac{t}{D}$ is the most important parameter and it is responsible of recirculation in the host artery (see [27]), but also curvature has a role (see [28]). The ratio $\frac{S}{D}$ becomes important if we freeze $\frac{t}{D}$ and so the graft angle θ .

Figure 14 (left) shows a comparison between the vorticity functional output, defined as $s(\mu) = \int_{\Omega_d} (\frac{\partial u}{\partial x} - \frac{\partial v}{\partial y}) d\Omega$, calculated with Stokes and Navier-Stokes equations. We can see that the Stokes model is a good approximation only if the ratio $\frac{t}{D}$ is less than unity and this is our case, otherwise if the bypass diameter t is too small with respect to the arterial diameter D a strong recirculation arises in the host vessel and also vorticity increases considerably. These phenomena are not well captured by the Stokes linearized model. Usually the value of the quantity $\frac{t}{D}$ is in the range $[0.85 - 0.96]$. This test gives us important information about the fidelity of our model and it allows a generalization of results available in the literature, especially provided by experimental research activity and surgical experience.

Figure 14 (right) shows the behavior of vorticity where we vary the curvature of the upstream (inflow) geometry. Increasing the curvature v the vorticity diminishes: this behavior can be explained by the fact that curvature is guiding the flow more smoothly. An interesting analysis can be obtained introducing the *Dean* number, representing the ratio of the square root of the product of the inertial and centrifugal forces to the viscous forces, defined as follows

$$De = 4 \left[\frac{D}{R} \right]^{\frac{1}{2}} Re, \quad (8.70)$$

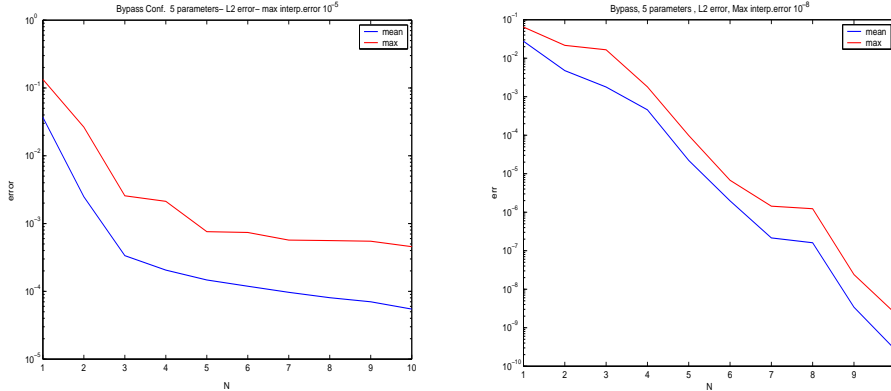


Figure 13: L^2 relative errors on pressure with different ϵ_{max} interpolation error imposed on all $g_M^j(x, \mu)$ (testing hundreds of configurations with 5 different parameters varying).

where R is the radius of curvature and Re the Reynolds number. See also Doorly and Sherwin [30]. If the curvature is zero the Dean number is zero too. In the case we have considered, the range of the Dean number was $[0, 2.31] \cdot Re$. By increasing the Dean number (and so *curvature*, the inverse of the curvature radius) makes the maximum of the $2D$ velocity profile to increase, but at the same time this maximum is displaced away from the center of curvature. Note that $De = 0$ corresponds to a case in which we have a centered velocity profile of *Hagen-Poiseuille* type. In our case the displacement of the peak velocity profile allows the blood to be driven into the host vessel more smoothly and to better adapt the upstream inflow condition at the junction geometry. In our case the critical zone of the bypass near the upper wall has lower mean velocity. The introduction of the upstream curvature has been discussed also in Papaharilaou, Doorly and Sherwin [16]. Results in Figure 14 (right) refers to a graft angle of 45 degree and a ratio $\frac{t}{D} = 1$.

9 Conclusions

We have extended the use of reduced basis methodology to non-linear problems in domains with non-affine parametric dependence. This generalization has allowed us to approximate flows in parametrized domains, e.g. blood flows in arterial bypasses depending on physical and geometrical parameters. The aim has been to provide (a) a sensitivity analysis for relevant geometrical and physical quantities and (b) rapid and reliable prediction of integral functional outputs (such as fluid mechanics indexes). The goal of this investigation is (i) to develop numerical methods for optimization and design in fluid mechanics, and (ii) to provide an input-output relationship led by models with lower complexity and computational costs than the complete solution of fluid dynamics equations by

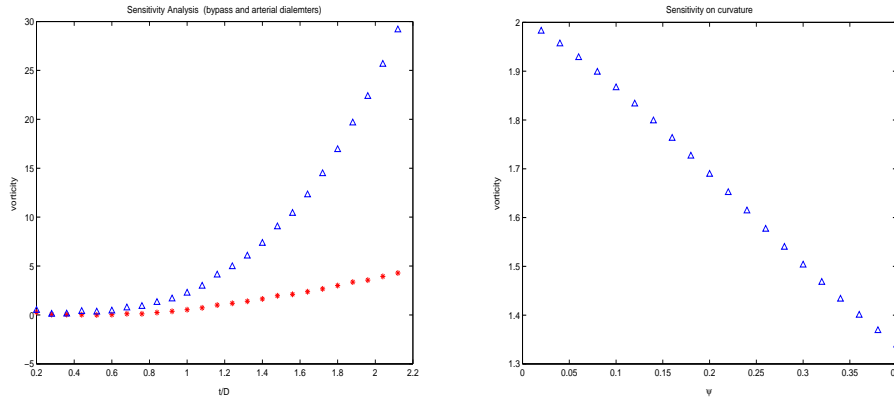


Figure 14: Distributed vorticity [m^2s^{-1}] versus $\frac{t}{D}$ and comparison between Stokes (*) and Navier-Stokes (Δ) flows (left); distributed vorticity [m^2s^{-1}] and curvature (right).

a classical finite element method.

When we are considering problems with an increasing complexity, such as the ones with non-linearities and non-affine parametrization, the use of reduced basis method becomes even more competitive and computational savings are more relevant.

10 Acknowledgements

We are very grateful to Prof. A. T. Patera and Dr. K. Veroy of MIT for suggestions, very helpful discussions, comments and insights. We thank Prof. F. Saleri (MOX-Politecnico di Milano) for providing the original finite element Navier-Stokes solver. G. Rozza acknowledges the support provided through the European Community's Human Potential Programme under contract HPRN-CT-2002-00270 HaeMOdel and through Swiss National Science Foundation (PBEL2-111646). This work has also been supported by Italian MIUR Cofin2005 "Numerical modelling in fluid dynamics with application to the cardiovascular system and environment".

References

- [1] M. Barrault, Y. Maday, N.C. Nguyen and A.T.Patera. *An "empirical interpolation" method: application to efficient reduced-basis discretization of partial differential equations*. C. R. Acad. Sci. Paris, Analyse Numerique, Serie I, 2004, Vol. 339, pp. 667–672.

- [2] F. Brezzi, M. Fortin. *Mixed and Hybrid Finite Element Methods*. Springer and Verlag, New York, 1991.
- [3] J. Burkardt. *Flow optimization using sensitivities*. Preprint, School of Computational Science, Florida State University, submitted, 2005.
- [4] J. Cahouet, J.P. Chabard. *Some fast 3D finite element solvers for the generalized Stokes problem*. International Journal Numerical Methods for Fluids, Vol. 8, No. 8 (1988), pp. 869–895.
- [5] C. Canuto, M.Y. Hussaini, A. Quarteroni, T.A. Zang. *Spectral Methods: Evolution to Complex Geometries and Applications to Fluid Dynamics*. Springer, Heildeberg, 2007.
- [6] G.P. Galdi. *An Introduction to the Mathematical Theory of the Navier-Stokes Equations, Volume II: Nonlinear Steady Problem*. Springer-Verlag, New York, 1994.
- [7] V. Girault, P.A. Raviart. *Finite Element Methods for Navier-Stokes Equations*. Springer-Verlag, Berlin, 1986.
- [8] M. Grepl, N.C. Nguyen, K. Veroy, A.T. Patera and G.R. Liu. *Certified rapid solution of parametrized partial differential equations for real-time applications*. 2nd Sandia Workshop on PDE-Constrained Optimization: toward real-time and online PDE-Constrained Optimization. SIAM, to appear, 2006.
- [9] P.M. Gresho, R.L. Sani. *Incompressible Flow and the Finite Elements Method*. J. Wiley, New York, 2000.
- [10] M.D. Gunzburger. *Finite Element Method for Viscous Incompressible Flows: A Guide to Theory, Practice, and Algorithms*. Academic Press, Boston, 1989.
- [11] M.D. Gunzburger. *Perspectives in Flow Control and Optimization*. SIAM, Advances in Design and Control, Philadelphia, 2003.
- [12] K. Ito, S.S. Ravindran. *A reduced-order method for simulation and control of fluid flow*. Journal of Computational Physics, Vol. 143, No. 2 (1998), pp. 403–425.
- [13] K. Ito, J.D. Schroeter. *Reduced order feedback synthesis for viscous incompressible flows*. Mathematical And Computer Modelling, Vol. 33, No. 1-3 (2001), pp. 173–192.
- [14] A.E. Løvgrén, Y. Maday, E.M. Rønquist, *A reduced basis method for the steady Navier-Stokes problem*. Preprint, 2006.

- [15] N.C. Nguyen, K. Veroy, A.T. Patera. Certified Real-Time Solution of Parametrized Partial Differential Equations. *Handbook of Materials Modeling*. R. Catlow, H. Shercliff and S. Yip Eds. Kluwer Academic Publishing (Springer), 2005.
- [16] Y. Papaharilaou, D.J. Doorly, S.J. Sherwin. *The influence of out-of-plane geometry on pulsatile flow within a distal end-to-side anastomosis*. Journal of Biomechanics, Vol. 35 (2002), pp. 1225–1239.
- [17] J.S. Peterson. *The reduced basis method for incompressible viscous flow calculations*. *SIAM J. Sci. Stat. Comput.*, Vol. 10, No. 4 (1989), pp. 777–786.
- [18] C. Prud’homme, D. Rovas, K. Veroy, Y. Maday, A.T. Patera and G. Turinici. *Reliable real-time solution of parametrized partial differential equations: reduced-basis output bound methods*. J. Fluids Engineering, Vol. 172 (2002), pp. 70–80.
- [19] C. Prud’homme, D. Rovas, K. Veroy and A.T. Patera. *Mathematical and computational framework for reliable real-time solution of parametrized partial differential equations*. *M²AN*, Mathematical Modelling and Numerical Analysis, Vol. 36, No. 5 (2002), pp. 747–771.
- [20] C. Prud’homme, A.T. Patera. *Reduced-basis output bounds for approximately parametrized elliptic coercive partial differential equations*. Computing and Visualization in Science, Vol. 6, No. 2-3 (2004), pp. 147–162.
- [21] A. Quarteroni, A. Valli. *Numerical Approximation of Partial Differential Equations*. Springer-Verlag, Berlin, 1994.
- [22] A. Quarteroni, R. Sacco, F. Saleri. *Numerical Mathematics*. Springer, New York, 2000.
- [23] D. Rovas. *Reduced-Basis Output Bound Methods for Parametrized Partial Differential Equations*. PhD Thesis, MIT, Massachusetts Institute of Technology (February 2003).
- [24] G. Rozza, K. Veroy. *On the stability of reduced basis method for Stokes equations in parametrized domains*. To appear in Computer Methods in Applied Mechanics and Engineering, 2007.
- [25] G. Rozza. *Reduced basis methods for elliptic equations in sub-domains with a posteriori error bounds and adaptivity*. Applied Numerical Mathematics, Vol. 55, No. 4 (2005), pp. 403–424.
- [26] G. Rozza. *On optimization, control and shape design of an arterial bypass*. International Journal for Numerical Methods in Fluids, Vol. 47, No. 10-11 (2005), pp. 1411–1419.

- [27] G. Rozza. *Real time reduced basis techniques for arterial bypass geometries*. In K.J. Bathe (ed.), *Computational Fluid and Solid Mechanics*, Elsevier, 2005, pp. 1283–1287.
- [28] G. Rozza. *Shape Design by Optimal Flow Control and Reduced Basis Techniques: Applications to Bypass Configurations in Haemodynamics*. PhD Thesis No.3400, EPFL, Ecole Polytechnique Fédérale de Lausanne, 2005.
- [29] G. Rozza. *Reduced basis methods for Stokes equations in domains with non-affine parameter dependence*. EPFL-IACS report 06.2005, submitted 2005.
- [30] S.J. Sherwin, D.J. Doorly. *Flow dynamics within model distal arterial bypass graft*. *Advances in Fluid Mechanics*, Vol. 34 (2003), pp. 327–374.
- [31] I.J. Sobey. *On flow furrowed channels. Part 1. Calculated flow pattern*. *Journal of Fluid Mechanics*, Vol. 96, Part I (1980), pp. 1–26.
- [32] K.D. Stephanoff, I.J. Sobey, B.J. Bellhouse. *On flow through furrowed channels. Part 2. Observed flow patterns*. *Journal of Fluid Mechanics*, Vol. 96, Part I (1980), pp. 27–32.
- [33] R. Temam. *Navier-Stokes Equations: Theory and Numerical Analysis*. North-Holland, Amsterdam, 1984.
- [34] K. Veroy and A.T. Patera. *Certified real-time solution of the parametrized steady incompressible Navier-Stokes equations; Rigorous reduced-basis a posteriori error bounds*. *International Journal Numerical Methods for Fluids*, Vol. 47, No. 8-9 (2005), pp. 773–788.
- [35] K. Veroy and A.T. Patera. *Reduced-basis approximation of the viscosity-parametrized incompressible Navier-Stokes equation: Rigorous a posteriori error bounds*. In *Proceedings Singapore-MIT Alliance Symposium*, January 2004.